

เสวต สมนึกพงษ์ : การระบุม่านตาบนพื้นฐานของสัมประสิทธิ์ฟูเรียร์และการแยกค่าเอกฐาน. (Iris Identification based on Fourier Coefficients and Singular Value Decomposition) อ. ที่ปรึกษาวิทยานิพนธ์หลัก: อ.ดร.ศุภกานต์ พิมลธเรศ อ. ที่ปรึกษาวิทยานิพนธ์ร่วม: ผศ.ดร.ศรันญา มณีโรจน์, 72 หน้า.

ในปัจจุบันการระบุตัวตนบุคคลนั้นเป็นสิ่งสำคัญมากเพื่อที่จะระบุตัวตนบนแอปพลิเคชันที่เกี่ยวกับการรักษาความปลอดภัยนั้น การพิสูจน์อัตลักษณ์จำเป็นต้องถูกนำมาวิเคราะห์ การพิสูจน์อัตลักษณ์นั้นเป็นสิ่งที่แพร่หลายอย่างมากในการระบุตัวตน ซึ่งในปัจจุบัน ข้อมูลอัตลักษณ์ที่ถูกนำมาใช้มีอยู่หลายแบบ ในงานวิจัยนี้ ม่านตา ซึ่งเป็นอัตลักษณ์อย่างหนึ่งได้ถูกนำมาใช้ในการพิสูจน์เพราะความมีเอกลักษณ์เฉพาะตัวสูงมาก เมื่อไม่นานมานี้ ปัญหาของระบบการพิสูจน์อัตลักษณ์ด้วยม่านตาต่างๆคือข้อจำกัดในการจัดเก็บข้อมูลในสภาพแวดล้อมที่แตกต่างกัน งานวิจัยนี้ได้นำเสนอระบบพิสูจน์อัตลักษณ์ด้วยม่านตาแบบใช้พีเจอร์ขนาดเล็กซึ่งเป็นสาเหตุทำให้เกิดความซับซ้อนในการจัดเก็บข้อมูล สำหรับการทดลองนี้ ข้อมูลม่านตาจะถูกนำเสนอในโดเมนของความถี่และใช้โครงข่ายประสาทเทียมในการแยกข้อมูล ซึ่งอันดับแรก อัลกอริทึมการแปลงฟูเรียร์แบบรวดเร็ว (Fast Fourier Transform) จะถูกนำมาใช้เพื่อคำนวณหาค่าสัมประสิทธิ์ฟูเรียร์แบบไม่ต่อเนื่อง (Discrete Fourier Coefficient) ในโดเมนของความถี่ เมื่อข้อมูลม่านตาถูกแปลงเป็นเมตริกซ์ในโดเมนของความถี่แล้ว เวกเตอร์ทั้งหมดเหล่านี้ จะกลายเป็นข้อมูลนำเข้าให้กับโครงข่ายประสาทเทียมเพื่อการแยกข้อมูล ด้วยวิธีการนี้แล้ว ผลลัพธ์ที่ได้รับคือ ขนาดของพีเจอร์จะมีขนาดเล็กเมื่อเปรียบเทียบกับเทคนิคอื่นๆ อีกทั้งความถูกต้องในการแยกข้อมูลนั้นอยู่ในระดับที่ยอมรับได้เมื่อเปรียบเทียบกับเทคนิคอื่น

ภาควิชา : คณิตศาสตร์และวิทยาการคอมพิวเตอร์ ลายมือชื่อนิติ.....

สาขาวิชา : วิทยาการคอมพิวเตอร์และสารสนเทศ ลายมือชื่อ อ. ที่ปรึกษาวิทยานิพนธ์หลัก.....

ปีการศึกษา : 2554..... ลายมือชื่อ อ. ที่ปรึกษาวิทยานิพนธ์ร่วม.....

5273614023 : MAJOR COMPUTER SCIENCE AND INFORMATION

KEYWORDS : BIOMETRIC / FAST FOURIER TRANSFORM / SINGULAR VALUE
DECOMPOSITION / IRIS RECOGNITION

SAWET SOMNUGPONG : IRIS IDENTIFICATION BASED ON FOURIER
COEFFICIENTS AND SINGULAR VALUE DECOMPOSITION.

ADVISOR: SUPHAKANT PHIMOLTARES, Ph.D.,

CO-ADVISOR : ASST. PROF. SARANYA MANEEROJ, Ph.D., 72 pp.

Nowadays, both personal identification and classification are very important. In order to identify the person for some security applications, physical or behavior-based characteristics of individuals with high uniqueness might be analyzed. Biometric becomes the mostly used in personal identification purpose. There are many types of biometric information currently used. In this research, iris, one kind of personal characteristics is considered because of its uniqueness and collectable. Recently, the problem of various iris recognition systems is the limitation of space to store the data in a variety of environments. This research proposes the iris recognition system with small-size of feature vector causing a reduction in space complexity term. For this experiment, each iris is presented in terms of frequency domain, and based on neural network classification model. First, Fast Fourier Transform (FFT) is used to compute the Discrete Fourier Coefficients of iris data in frequency domain. Once the iris data was transformed into frequency-domain matrix, Singular Value Decomposition (SVD) is used to reduce a size of the complex matrix to single vector. All of these vectors would be input for neural networks for the classification step. With this approach, the merit of our technique is that size of feature vector is smaller than that of other techniques with the acceptable level of accuracy when compared with other existing techniques.

Department : Mathematics and Computer Science

Student's Signature

Field of Study : Computer Science and Information

Advisor's Signature

Academic Year : 2011.....

Co-advisor's Signature

CHAPTER I

INTRODUCTION

1.1 Motivation

With the increasing of demand in many organization or security systems, both personal identification and verification are very crucial. Some organization or systems provide their security by using various approaches, such as password, key card, RFID, etc. But the legacy security systems seem not good enough while comparing with the growth of technology. In order to improve the security to compete with the high growth rate of terrorist and malicious people, the efficient security system must be provided in various organizations. The common problem of the security system is holding some key to identify ourselves to access in the system. The most crucial problem of holding some key is that the key might be stolen by those terrorists or malicious people.

From these reasons, the outcome idea is the research about integrating the key with human body. Biometric is one kind of the integration among keys to access into the system with the person who has the privilege. The key is special characteristic in personal body which can identify a person by itself. These characteristics have its own very high of uniqueness and hard to be stolen as compared to the legacy key in the old security system.

There are two kinds of identification by using biometric data, which are based on physical appearance or behavior in a personal body such as, voice, signature, and human movement. For physical based appearance, there are many types such as palm print, fingerprint, face, keystroke, voice, and retina. Each of which has its own characteristic, palm print characteristics are the pattern of ridges in personal palm combining with shape of palm and distance between joints of fingers. Face characteristics consist of shape of face, distance between eyebrows, nose and shape of lip. The voice characteristic is signal in terms of frequency. All of mentioned biometric

has level of uniqueness and stability. Some would be changed while the time has passed.

From the reason mentioned, the biometric data which is used in this research must be stable and unique enough to use in some particular system, which provides very high security level.

Iris is one of the personal characteristics, which is located in a human eye between the pupil region and sclera region. The pattern of iris normally represents in ring shape, and the analysis of texture in ring shape area is needed in order to identify people. The stability of iris is very high, because the texture of iris would not be changed according to time. From these reasons, iris identification becomes very popular and active research in a present.

There are a lot of common problems in iris identification, size of feature, time consuming, accuracy rate, etc. Many researchers focus on accuracy and don't care any other factors. Some of the research is not appropriate because of a limitation of a particular situation, for example, some research obtains high-accuracy rate while sizes of features are very large. This directly affects to a particular device which has a limitation of space and use long time in processing while it is practically used. For this reason, this research intends to develop the iris recognition system using a small size of features while the accuracy is in acceptable level.

1.2 Problem Description

1. What are new features suitable for the iris recognition system?
2. What technique will be used to perform the main system in the iris recognition?
3. How to reduce the size of feature vector?
4. How to evaluate experimental results?

1.3 Literature Review

In recent survey, there are many methods of iris feature extraction in the iris identification system. Some of them emphasizes accuracy rate of recognition, and some of them emphasizes time reduction while processing as follows:

1.3.1 Kekre method

Kekre [1] proposed Iris Recognition Using Vector Quantization. This method uses vector quantization to compress the iris data, and then Euclidean distance is used as a dissimilarity measure between iris images. The advantage point is that the overall process performs faster than the other current techniques. In contrast, the disadvantage point is that iris image contains a lot of noise, and its recognition rate provided 81.25% - 89.10%. This research applies using vector quantization to compress the iris data, and using LBG, KPE and KFCG clustering in order to generate feature vector.

1.3.1.1 Vector Quantization

Vector Quantization is an efficient technique for data compression and very widely used in various applications such as index compression [2], speech recognition, face detection [3], and many real time applications. Most of iris recognition system performance is depends on preprocessing, and localization of the iris. For this method, Kekre discusses an iris identification system which does not need any preprocessing step. Iris image is quantized as a feature vector, then three clustering algorithm is used namely Linde-Buzo-Gray algorithm (LBG), Kekre's Proportionate Error algorithm (KPE) and Kekre's Fast Codebook Generation algorithm (KFCG).

1.3.1.2 Linde-Bruzo-Gray Clustering (LBG)

For this algorithm, iris data is quantized into two-dimensional vector space. Each point in figure represents two consecutive pixels, and image is divided into two blocks. Centroid is computed as the first code vector C_1 for the training set as Figure 1.1a. The disadvantage of this algorithm is the expansion of clustering is +135

degrees to horizontal axis in two-dimensional case. This result is inefficient clustering [4].

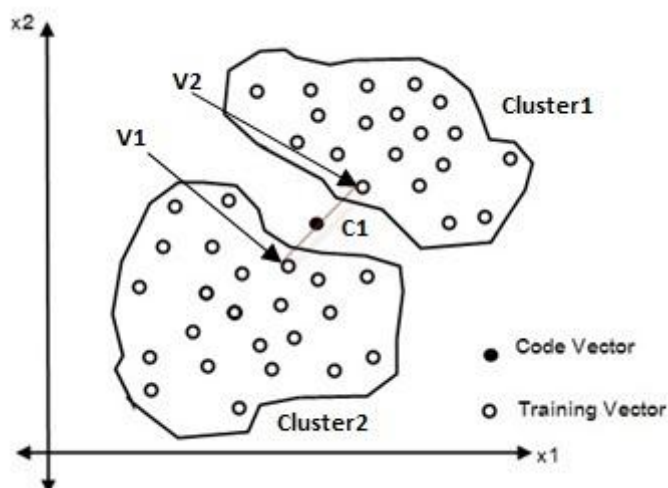


Figure 1.1a: LBG for two dimension case in 1st iteration

1.3.1.3 Kekrel's proportionate Error algorithm (KPE)

This algorithm emphasizes on fixing the drawback of LBG clustering. The proportionate error is added to the centroid to generate two vectors v_1 and v_2 . In this algorithm, the proportionate error is used in order to prevent neither v_1 or v_2 go beyond the training vector space.

1.3.1.4 Kekre's Fast Codebook Generation algorithm (KFCG)

The advantage of this algorithm is time reduction while generating codebook. First step, there is one cluster with entire training vectors, and the centroid is computed as C_1 . In the first iteration of algorithm, the cluster form is separated by comparing between first element of training vector and code vector C_1 . The vector X_i is grouped into cluster one if $X_{i1} < C_{11}$ otherwise vector X_i is grouped into cluster two as shown Figure 1.2a. Second iteration, the cluster one is separated into two subclusters by comparing the second element X_{i2} of vector X_i in cluster one with second element of code vector. Cluster two is separated into two subclusters by comparing the second

element X_{i2} of vector X_i in cluster two with the second element of code vector as shown in Figure 1.2b.

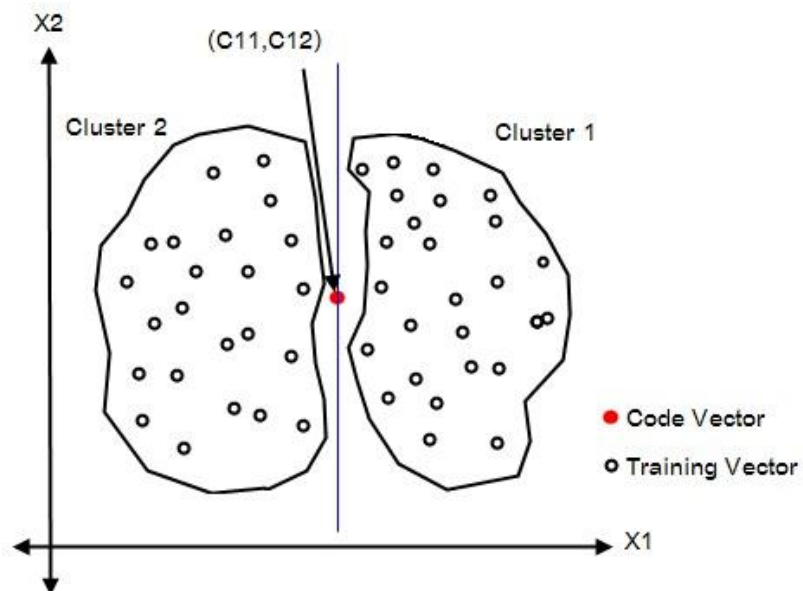


Figure 1.2a: First iteration of KFCG clustering algorithm

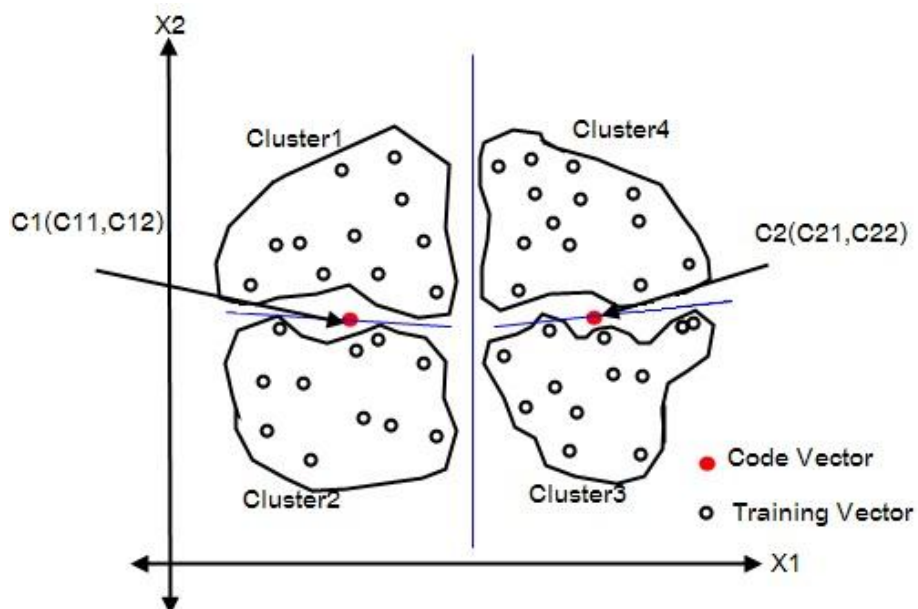


Figure 1.2b: Second iteration of KFCG clustering algorithm

In this method, Kekre define the codebook size as 16, and the feature vector has 16x12 numbers of elements. The following are the steps to generate the feature vector database

- Image is divided into window size 2x2 pixels.
- These values are rearranged into row order to get 12 values per vector as a training set.
- Compute centroid (code vector) of the cluster.
- Apply LBG/KPE/KFCG algorithm to generate codebook size 16.
- Finally, code book size 16x12 which is very small is obtained, the Euclidean distance is applied to use as similarity measure as following equation.

$$ED = \sqrt{\sum_{i=1}^n (V_{pi} - V_{qi})^2} \quad (1)$$

where V_{pi} and V_{qi} are feature i of image p and query q respectively

Algorithm	% Accuracy		
	Left eye	Right eye	Total Accuracy
LBG	78.13%	84.38%	81.25%
KPE	82.81%	84.38%	83.59%
KFCG	87.50%	90.63%	89.10%

Table 1.1: Illustration of the classification accuracy by Kekre's method

1.3.2 Boles method

For Boles's method [5], the process of feature extraction starts by localizing pupil region in iris image, which applying any edge detection technique. The centroid of pupil region is determined as the main point to extract feature of iris. The gray scale values on the contour of virtual circle, which are centered at the centroid of pupil are record and stored. This dataset is represented in terms of iris signature. The extracted iris signature from any image must be normalized to have the same length which is 250 as shown in Figure 1.3a. The drawback of this method is that just one virtual circle around pupil is not unique enough to represent the iris signature. The accuracy of this method is 92.64%.

1.3.2.1 Zero-Crossing generation

After the iris signature from virtual circle is obtained, the zero-crossing is generated from normalized iris signature as Figure 1.3c. The zero-crossing is a periodic signal. Hence, the representation is independent from starting point on iris virtual circle

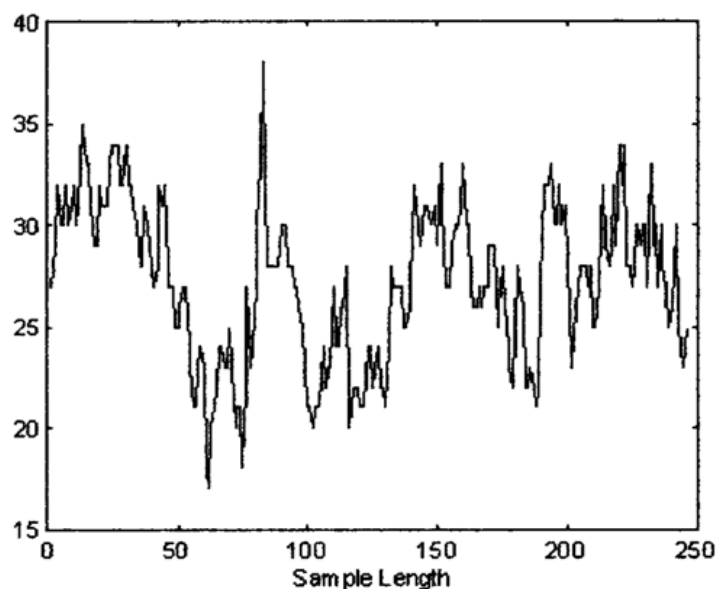


Figure 1.3a: Sample iris signature from image

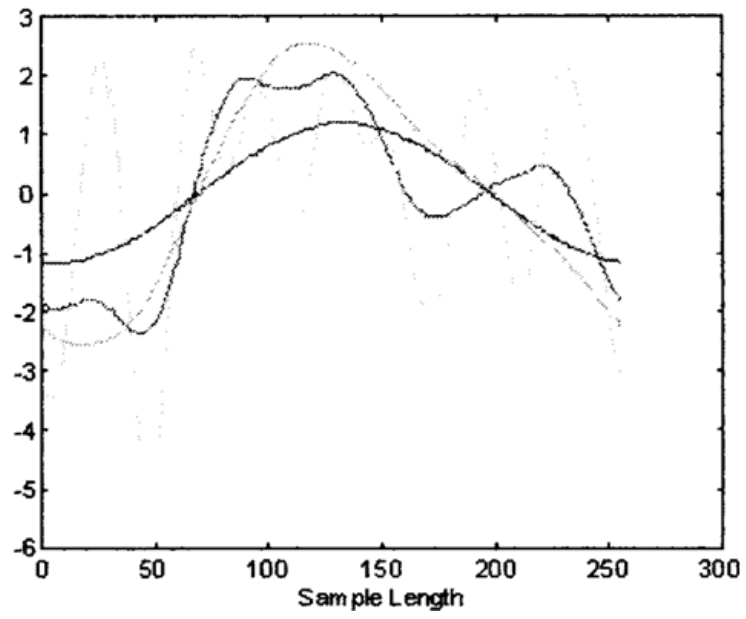


Figure 1.3b: Lowest four resolution levels of wavelet transform

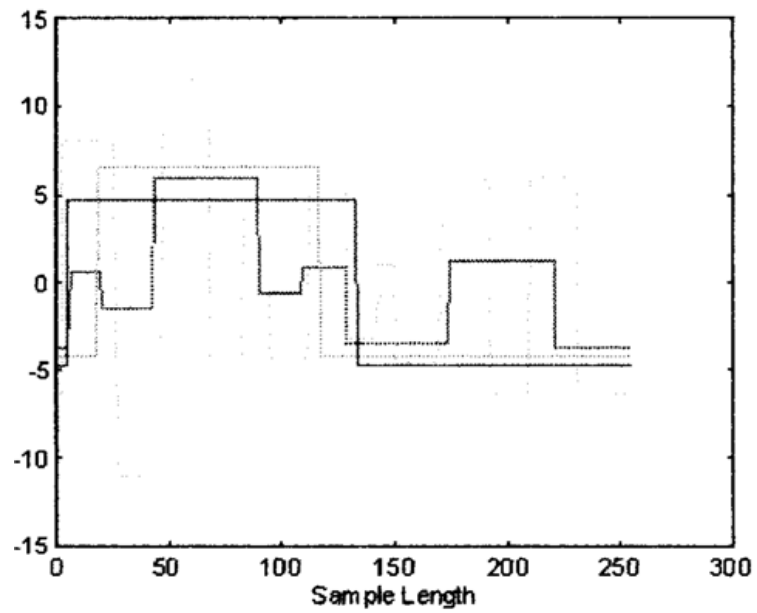


Figure 1.3c: Zero-Crossing representation of iris

Wavelet transformation is used to decompose the signal into a set of signal with various levels. The quality of signal at better resolution level is directly affected by noise. In Figure 1.3b, only four low-resolution levels are used in order to reduce this effect on zero-crossing representation. This makes better performance and robust to noisy environment.

1.3.3 Daugman Method

From Kekre and Bole methods, they emphasize on small size of feature while dropping the accuracy rate of recognition. Because of the information which used to extract the iris data is not good enough. For Daugman's method [6], the iris pattern is extracted into 2D Gabor wavelets to generate iris code, and then Hamming Distance is used to compute the dissimilarity between two iris codes. The accuracy rate of this method is 100%.

1.3.3.1 2D Gabor Wavelet

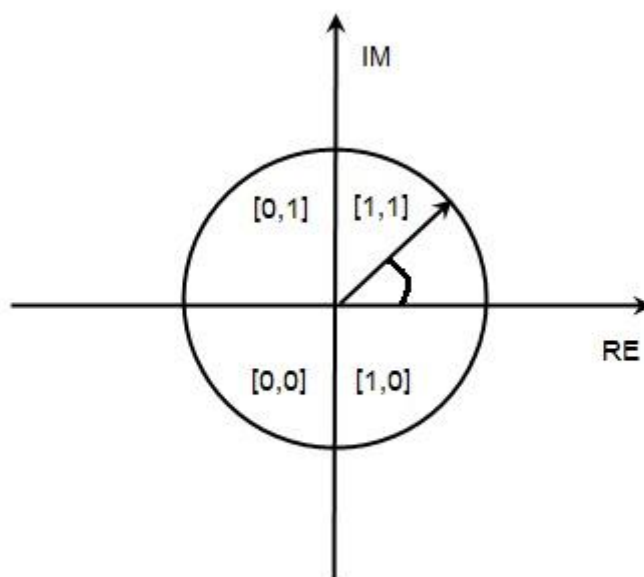


Figure 1.4a: The phase demodulation used to encode iris pattern

Local regions of an iris is computed as equation (2) and projected onto quadrature 2D Gabor wavelets, the complex-valued coefficients of real and imaginary parts is generated as a phasor coordinate in complex plane. The angle of each phasor is quantized to one of the four quadrants as Figure 1.4a, and two bits are used to represent in each quadrant. This encoding is repeated continuously to all iris regions with a lot of wavelet sizes, frequencies, and orientations in order to extract iris code size 2048 bits.

$$h_{(\text{Re,Im})} = \underset{(\text{Re,Im})}{\text{sgn}} \int_p \int_\phi I(\rho, \phi) e^{-i\omega(\theta_0 - \phi)} e^{-(r_0 - \rho)^2 / \alpha^2} e^{-(\theta_0 - \phi)^2 / \beta^2} \rho d\rho d\phi \quad (2)$$

where

- $h_{(\text{Re,Im})}$ is the complex-valued bit in real and imaginary. The value is either 0 or 1 (sgn) depending on the sign of 2D integral
- $I(\rho, \phi)$ is the iris image in polar system
- α and β are the multi-scale 2D wavelet size parameter
- ω is wavelet frequency
- (r_0, θ_0) represent polar coordinate of each iris region where the phasor coordinates are computed

1.3.3.1 Hamming Distance

The matching step of this method is based on Boolean Exclusive-OR operation (XOR). The operation performs bit by bit to set iris code which obtained from applying 2D Gabor Wavelet.

$$HD = \frac{\|(\text{code}A \otimes \text{code}B) \cap \text{mask}A \cap \text{mask}B\|}{\|\text{mask}A \cap \text{mask}B\|} \quad (3)$$

where

- *codeA* is the testing iris code
- *codeB* is the iris code template
- *maskA* is a mask bit of testing vector
- *maskB* is a mask bit of template vector

From literature review, some of works realize in size reduction of feature vector, but drawback is the dropping of accuracy rate which causes from the information of iris is not good enough. The method which emphasize on the accuracy rate might use a lot of information to present iris characteristics, but size of a feature vector is very large. In this research, the idea that using the appropriate feature is consider to reduce size of feature and give more accuracy while compared with the method which use small size of feature.

1.4 The Objectives of Research

To develop a system of iris identification with small size of iris features.

1.5 Scope of Study

1. The iris identification system process is automatically operated.
2. The iris database template is obtained from CASIA database.
3. All iris images are represented in grey scale.
4. The size of original iris image is 320x240.

CHAPTER II

THEORETICAL FOUNDATION

This chapter explains about the theoretical foundation supporting in this research. It contains seven main topics: Circular Hough transform, Polar coordination transform, Histogram equalization, Window function, Fast Fourier transform algorithm, Singular Value Decomposition and Neural Classifier. The research is separated into three main phase, preprocessing phase, feature extraction phase, and classification phase.

The first phase performs the operation of locating iris region using Circular Hough Transform. Reformation of the obtained iris pattern from ring shape to rectangular shape using polar coordinate transform, then enhance the image using histogram equalization. The second phase explains the iris's feature extraction using Fast Fourier transform and size reduction using Singular Value Decomposition. The third phase contains the classification model using Back Propagation Neural network architecture.

2.1 Circular Hough Transform

Object identification in an image is one important task of computer vision. Some particular object in an image may be covered by noise [7]. In this research, circle region in an image is determined as an interest area. Iris pattern is normally represented in a circle form which is located between pupil region and sclera region. Circular Hough Transform is applied to find any circle object in sample image. The equation of a circle is explained as following:

$$r^2 = (x - a)^2 + (y - b)^2 \quad (4)$$

The parametric representation of the circle is:

$$\begin{aligned} x &= a + r \cos(\theta) \\ y &= b + r \sin(\theta) \end{aligned} \quad (5)$$

where

- a and b are center circle in x and y direction
- r is the radius

2.2 Polar Coordinate to Cartesian coordinate Transformation

Polar Coordinate Transform is a useful method to transform the particular image from Polar coordinate system to Cartesian coordinate system. In this research, this transformation is applied to transform the exact iris region in an original image from ring shape iris to rectangular shape. The definition of Polar coordinate system and Cartesian coordinate system are explained as follows.

2.2.1 Polar System

Polar system is a two-dimensional coordinate system of each point on a plane which is determined by distance from a point and an angle from direction. This coordinate system is normally represented in terms of coordinate (r, θ) . In the polar system, the origin point is called *pole* at the horizontal axis [8] as the following Figure 2.1a.

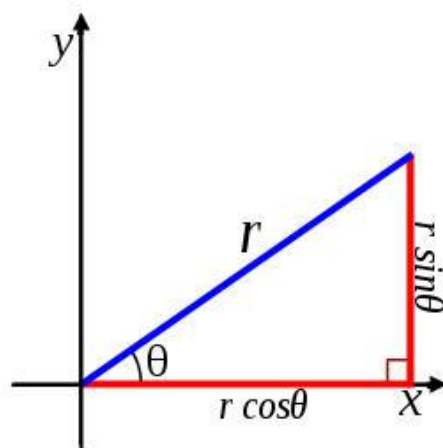


Figure 2.1a: Representation of Polar coordinate system

As the Figure 2.1a, a particular point is represented by (r, θ) where r represents the length of a straight line from the origin to particular point and θ represents the angle that particular point located base on polar axis. The r and θ components are commonly present used to the particular point as the radial coordinate as the angular coordinate respectively.

2.2.2 Cartesian System

The Cartesian system is a representation of each particular point on a plane by a pair of numerical coordinate where each of which is called coordinate x and coordinate y respectively. In order to determine the position of coordinate, x -axis and y -axis are determined as two main axis of coordinate system, and the cutting point between two axes is coordinate $(0,0)$ [9].

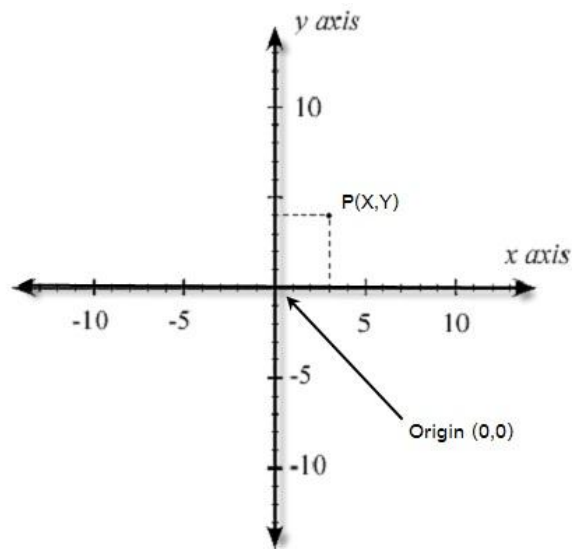


Figure 2.2a: Representation of Cartesian coordinate system

2.2.3 Transformation

Polar coordinate transform is the conversion from Polar coordinate to Cartesian coordinate (x, y) . The radial coordinate of particular point is denoted by r , and the angular is denoted by θ , while each particular point of Cartesian coordinate is represented in terms of (x, y) . The transformation from polar coordinate to Cartesian coordinate is relied on following equation.

$$\begin{aligned} x &= r \cos(\theta) \\ y &= r \sin(\theta) \end{aligned} \tag{6}$$

where

- x and y are components in Cartesian coordinate
- r and θ are radius and angle of specific point in Polar coordinate system, respectively.

The range of θ is from 0 – 360 degree. The following figure the relationship of particular point in Polar coordinate system and Cartesian coordinate system.

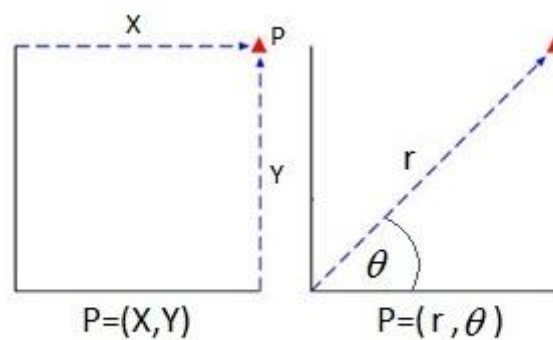


Figure 2.3a: The same position of specific point: Polar coordinate (right) and Cartesian coordinate (left)

2.3 Histogram Equalization

Histogram equalization is one of method widely applied in image processing. The main objective of method is contrast adjustment based on image histogram. The method performs balancing global contrast of image. This is very useful of the image for which some particular background and foreground are too bright or too dark.

2.4 Window Function

In signal processing, a window function is a mathematical function focusing on the value in specific interval. There are various applications using window function such as spectral analysis, filter design, etc.

Window function is mainly used to reduce the effect of leakage partially. The operation of window function in terms of multiplication is to smooth the sample signal at specific interval with cosine wave form. This research applies hanning window function with the iris signal for smoothing purpose. The hanning window is described as following equation.

$$w(n) = 0.5 \left(1 - \cos \left(2\pi \frac{n}{N} \right) \right), 0 \leq n \leq N \quad (7)$$

where

- N Represents the length of defined window in specific interval.
- n is the value of element in length N

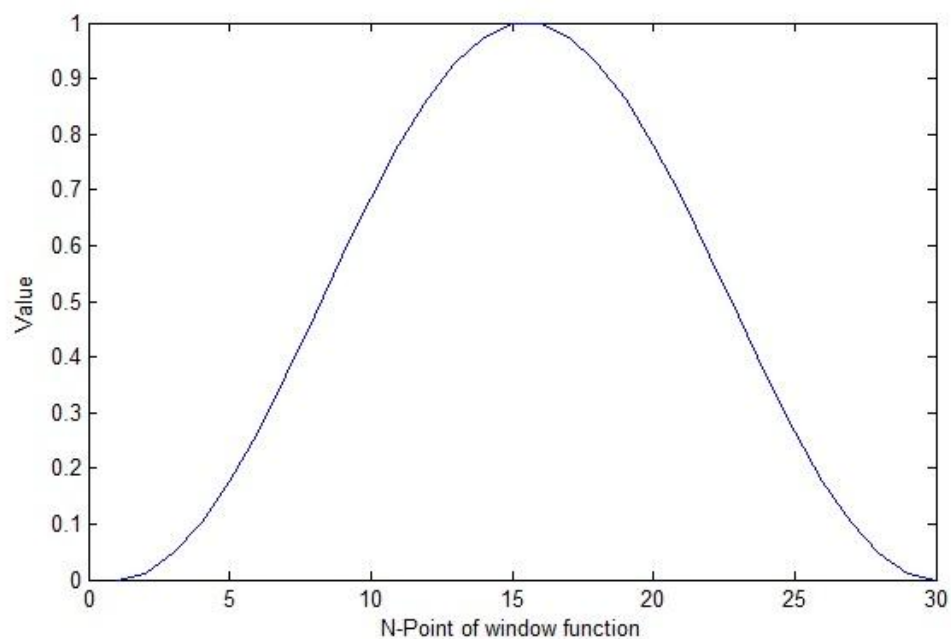


Figure 2.4a: Example plot of Hanning window length 30

2.5 Discrete Fourier Transform and Fast Fourier Transform Algorithm

Discrete Fourier Transform (DFT) is a one specific kind of discrete transform, and mostly used in frequency analysis. The operation is the transformation from original function to another function, which is called the frequency domain [10].

Fast Fourier Transform (FFT) is an efficient algorithm to compute the discrete Fourier transform and its inverse. FFT algorithm computes the DFT and produces the same result, but the different is that the computation speed is very fast

when compared with other algorithms. The sequence of N complex number x_0, \dots, x_{N-1} is transformed to another sequence of N complex number by following equation.

$$X_k = \sum_{n=0}^{N-1} x_n \cdot e^{-i2\pi \frac{k}{N}n} \quad (8)$$

and the inverse of discrete Fourier transform is given by:

$$x_n = \frac{1}{N} \sum_{k=0}^{N-1} X_k \cdot e^{+i2\pi \frac{k}{N}n} \quad (9)$$

where N is length of complex number

2.6 Singular Value Decomposition

Singular Value Decomposition (SVD) is a technique to decomposes a $m \times n$ matrix into one singular vector form [11]. SVD is very useful and popular in data compression in order to reducing size of data. The definition of SVD is described as following equation.

$$A = UDV^T \quad (10)$$

The relationship of an equation above is explained as

$$A = \begin{bmatrix} u_1 & u_2 & \dots & u_m \end{bmatrix}_{m \times m} \begin{bmatrix} d_1 & 0 & 0 & 0 \\ 0 & d_2 & 0 & 0 \\ 0 & 0 & \dots & 0 \\ 0 & 0 & 0 & d_{(m,n)} \end{bmatrix}_{m \times n} \begin{bmatrix} v_1^T \\ v_2^T \\ \vdots \\ v_n^T \end{bmatrix}_{n \times n} \quad (11)$$

where

- U is orthogonal vector of size $m \times m$
- V is orthogonal of $n \times n$

In this research, only diagonal matrix of D is used as a feature vector while other elements in D is zero.

2.7 Artificial Neural Network

An Artificial Neural Network (ANN) is a mathematical model for information processing. Ann is simulated to act like human brain for the capability in recognition of the particular object or other processings. In general, biological neural network consists of neurons, synapse, dendrite, and axon [12]. A biological neural is shown in Figure 2.5a, and artificial neural is shown in Figure 2.5b.

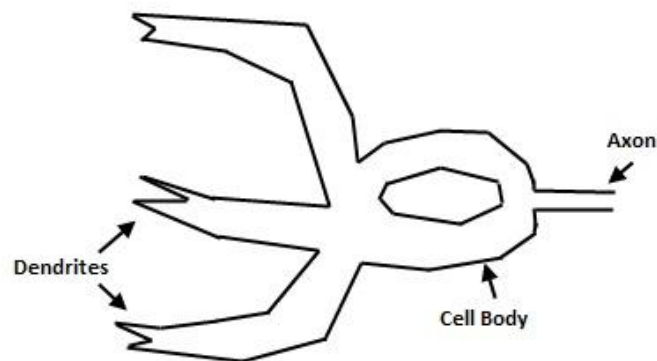


Figure 2.5a: Demonstration of biological neuron and its component.

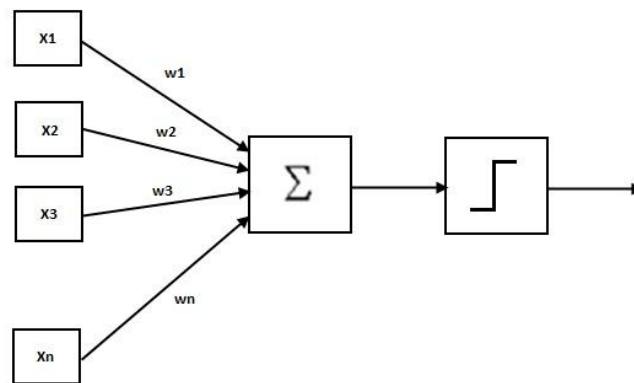


Figure 2.5b: Demonstration of Artificial Neuron and its component.

2.7.1 Back Propagation Algorithm

Back Propagation is one of the artificial neural network teaching methods. It is a supervised learning method. Normally, Back Propagation learning algorithm can be divided into two phases as following:

2.7.1.1 Phase 1: Propagation

Forward propagation of a training data set through neural network in order to generate output, and then propagate to next layer as Figure 2.6a.

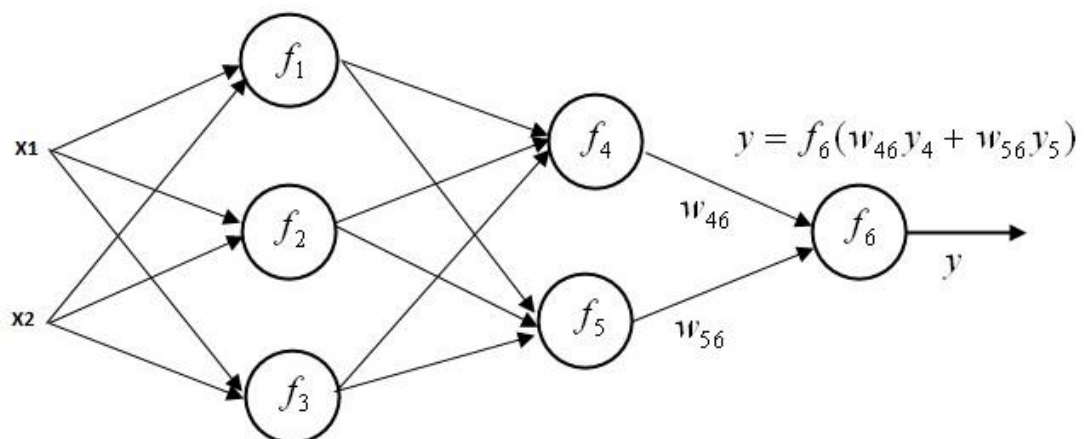


Figure 2.6a: Forward propagation of neural network.

At last node, subtract the output signal with the target value of training. The difference is called error signal of output neural. Propagate the error signals back by multiply each error signals with each weight of connection until the input node.

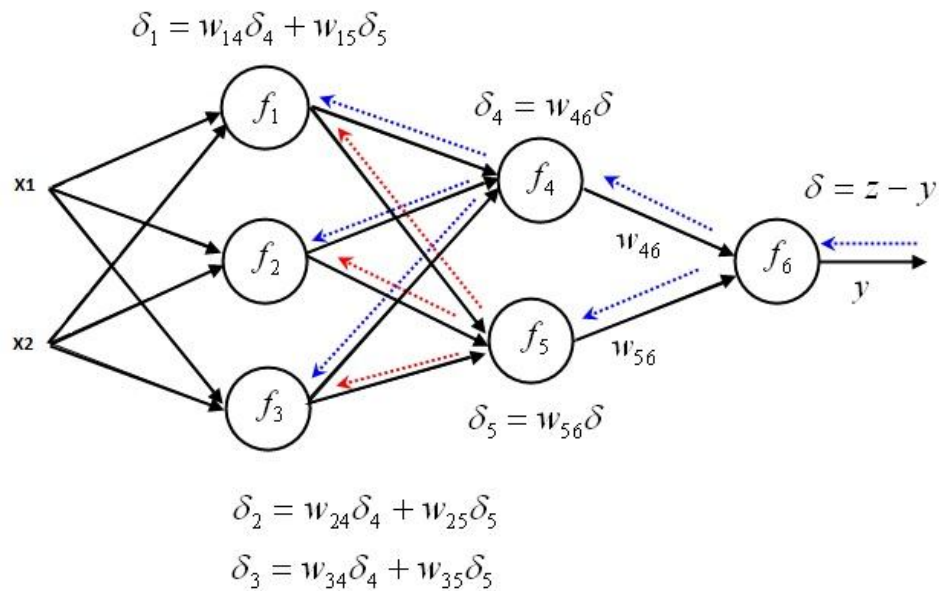


Figure 2.7a: Backward propagation of neural network.

2.7.1.2 Phase 2: Weight update

After the back propagation reach to the input node, the new weight of each connection will be modified in next step. The error signal of each node will be multiplied by derivative of activation function, input data and η where η is a learning rate that directly affects to network teaching speed. The weight updating will be calculated until the last node, and then the next iteration of training will go on.

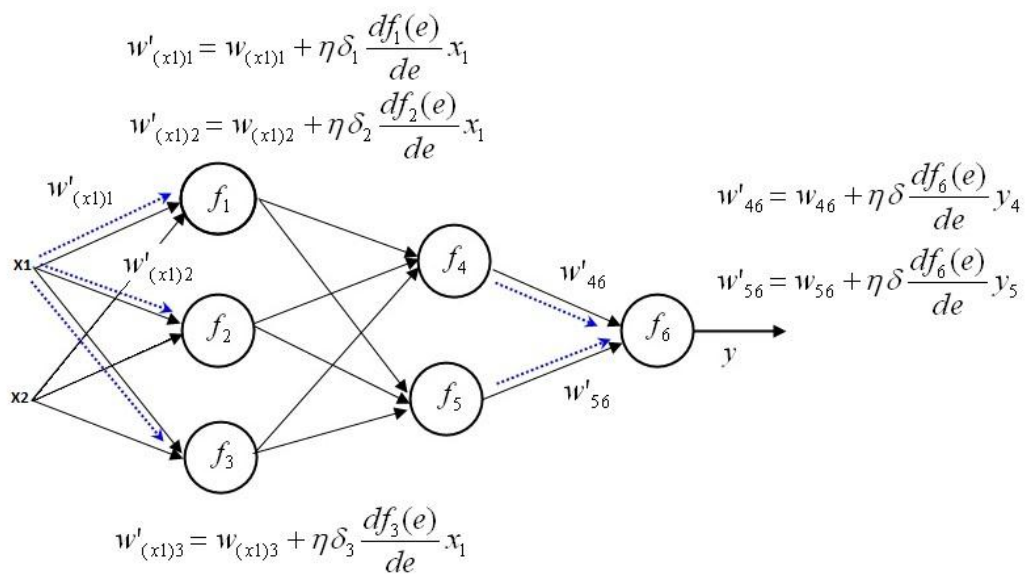


Figure 2.8a: Backward propagation of neural network.

CHAPTER III

METHODOLOGY

This chapter describes the methodology of the proposed method consisting of three phases. The first phase describes the preprocessing step of the image; this phase contains the iris localization for localizing the exact region of iris pattern and iris normalization, which performs in image enhancement. The second phase explains feature extraction method using Fast Fourier Transform algorithm to transform iris image from spatial domain into frequency domain, then reduce a size of features by applying Singular Value Decomposition. Last phase explains the classification process according to Back Propagation Neural Network as a learning model. The system is separated into three main steps consist of following:

- i. Preprocessing consist of iris localization, polar coordinate transformation, and iris normalization
- ii. Iris feature extraction using Fast Fourier Transform algorithm and Singular Value Decomposition
- iii. Classification using Back Propagation Neural Network

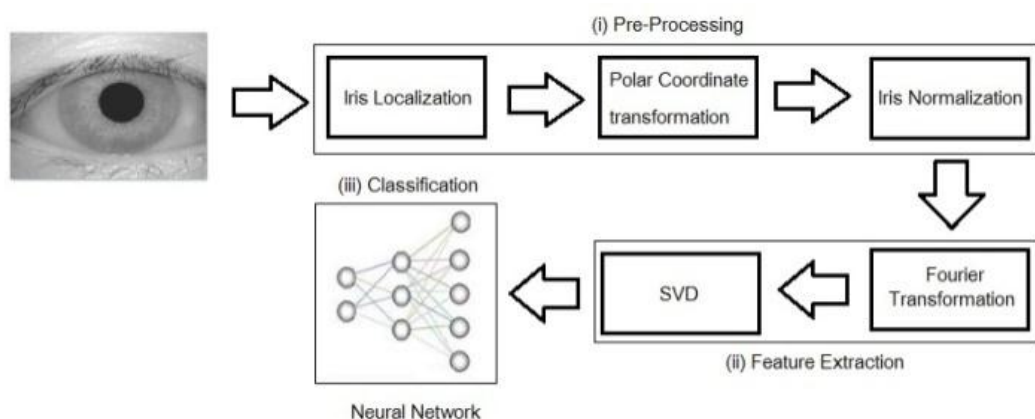


Figure 3.1a: Flow diagram of Iris identification system

3.1 Phase 1: Preprocessing Step

Preprocessing begins with localization step that localizes the exact iris region from original image, and also enhances the iris image in normalization step.

3.1.1 Iris Localization using Circular Hough Transform

Iris localization step is mainly performed in localizing an iris region in the image. Normally, human eye composed of eyelid, eyelashes, iris, pupil and sclera. The sclera is the white area in a human eye which is covered by several of blood vessel, pupil is the circle region located in center of human eye, and iris is the ring shape area which is located between sclera and pupil area. In order to utilize the iris in identification purpose, only exact iris region would be extracted distinctly from other eye composition.

Canny edge detection is applied to find edge image. This method operation is based on locating the local maximum of gradient value in an image. The gradient is calculated using the derivative of a Gaussian filter. Two threshold values are used to detect strong and weak edges, and only weak edges will be the output if it is connected to strong edges.

After the edge was detected (Figure 3.2b), Circular Hough Transform is used as a method to find the iris region. It is widely used to detect the inner boundary with high accuracy and can detect the object events covered by noise. From this advantage, Circular Hough Transform is applied to locate the iris region even though it is covered by eyelid and eyelash as following equation.

$$\begin{aligned}x &= x_0 + r \cos(\theta) \\ y &= y_0 + r \sin(\theta)\end{aligned}\tag{12}$$

The step of iris localization using CHT can be described as following:

```

Begin
max_ X = maximum x point
max_ Y = maximum y point
  For each edge point  $(x_i, y_j)$ 
    For  $(i = 0 : i \leq \text{max\_X} : i++)$ 
      For  $(j = 0 : j \leq \text{max\_Y} : j++)$ 
         $x = x_i + (r \cos(\theta))$ 
         $y = y_j + (r \sin(\theta))$ 
        Keep  $r, x$  and  $y$  in accumulator // Voting
      End
    End
  End
  Map the found parameter  $(r, x, y)$  corresponding to the maximum
  In accumulator back to the original image

```

Coordinate of center (x,y) and radius are obtained from this method. The center of inner circle and radius are obtained as shown in Figure 3.2c, outer circle is located immediate by the assumption that the texture area around pupil region which is covered by the circle with twice of pupil radius is useful to be analyzed.

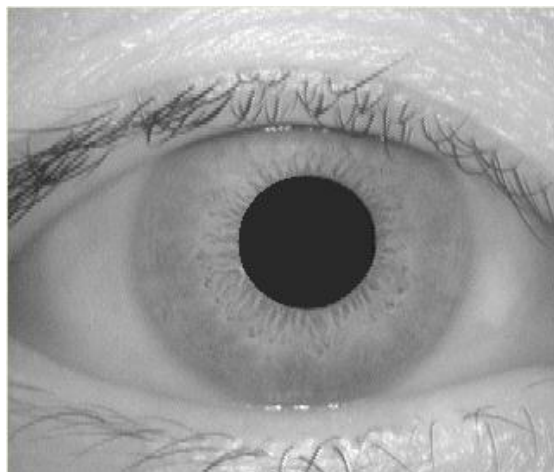


Figure 3.2a: Original gray scale iris image size 320x240

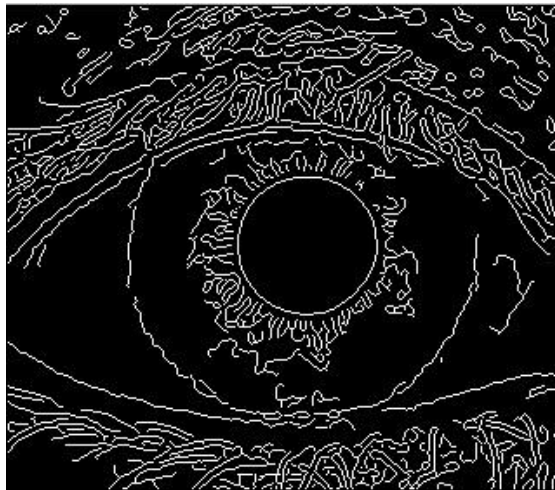


Figure 3.2b: Finding the edges using canny edge detector algorithm

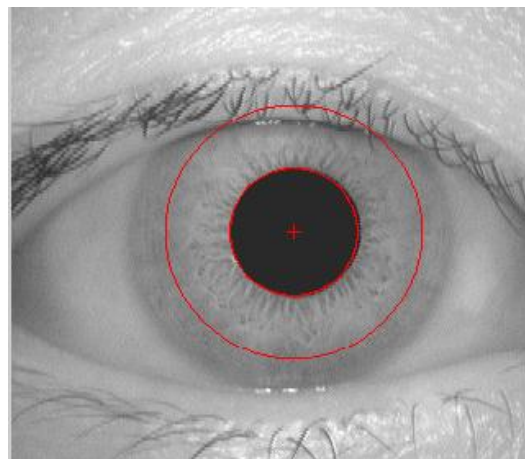


Figure 3.2c: Localization step for original iris image

In addition, the variation of ridges of iris contains a high amount of information in terms of frequency. This is a reason why Fast Fourier Transform (FFT) is required in the feature extraction process. In other words, texture around pupil region is significant enough to represent the characteristic of iris. The center of inner circle and radius are obtained, outer circle is located immediately by the assumption that the texture area around pupil region which is covered by the circle with twice of pupil radius is useful to be analyzed.

3.1.2 Polar Coordinate Transformation

Polar Coordinate Transformation mainly performs the transformation of original iris image from Polar coordinate system which represented in (r, θ) form into Cartesian coordinate system (x, y) . In Polar coordinate system, θ represents the angular coordinate and r represents the radial coordinate of particular point.

From previous phase, two parameters are obtained which are center coordinate of pupil and radii of inner circle and outer circle. These two parameters are necessary in this transformation phase.

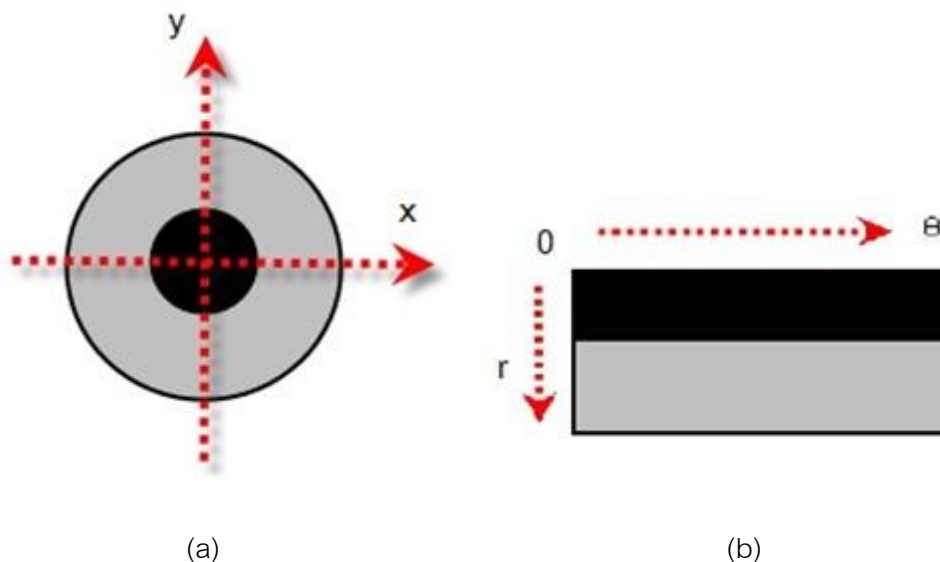
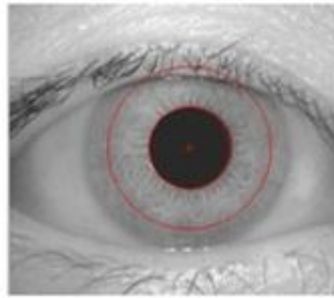


Figure 3.3a: The transformation step from ring shape to rectangular shape

(a) Transformation step (b) Transformation example.



(a)



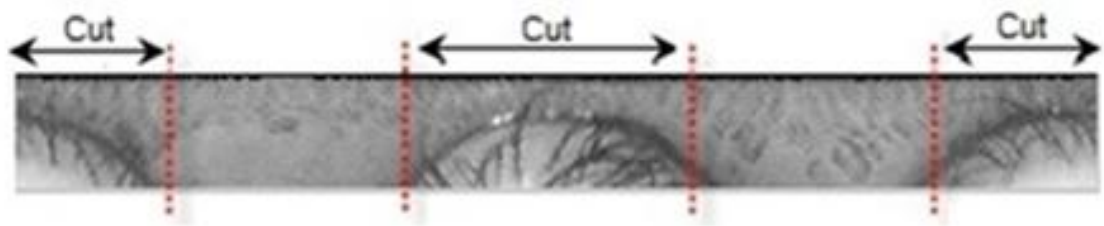
(b)

Figure 3.3b: Polar coordinate transformation of original iris

(a) Iris pattern in original eye image (b) Iris pattern after transformation

3.1.3 Normalization

The beginning of this process is eliminating the unnecessary regions, including eyelids and eyelash. Furthermore, to enhance the image contrast, histogram equalization is adopted to balance image intensity of entire image. The method is appropriate with an image which is too dark or too bright. This could distinguish the pattern of iris more obviously.



(a)



(b)

Figure 3.4a: Iris region after transformation with preparing to cut-off unnecessary part

(a) Before cut-off unnecessary part (b) After cut-off unnecessary part

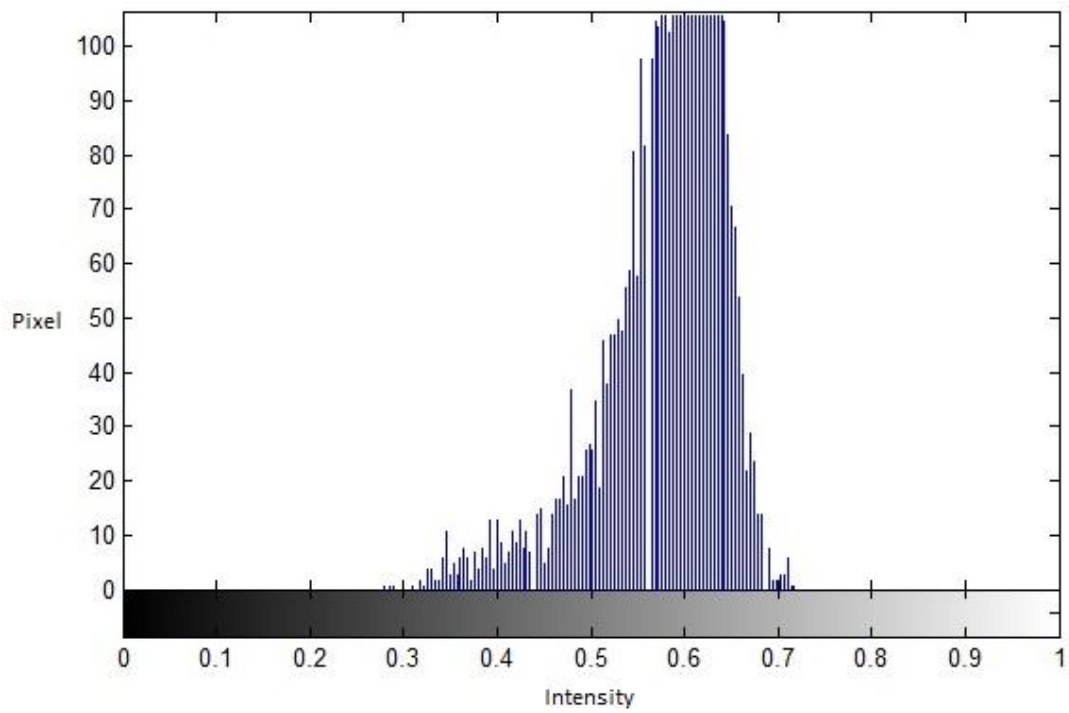


Figure 3.5a: Histogram of image before applying Histogram equalization

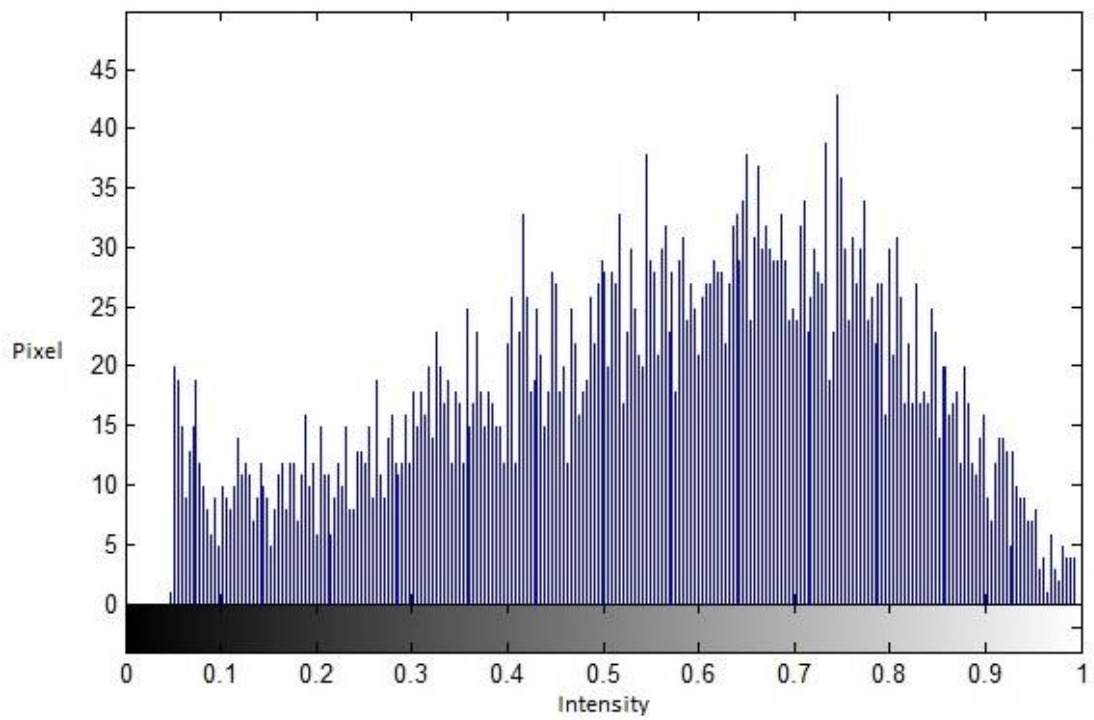


Figure 3.5b: Histogram of image after applying Histogram equalization



(a)



(b)

Figure 3.6a: Iris region after cut-off unnecessary part with preparing to apply Histogram equalization (a) Before applying Histogram equalization (b) After Before applying Histogram equalization

Figure 3.6a, the image contrast is enhanced using histogram equalization, eyelids and eyelashes are removed to prevent noisy effect whilst the real region of iris data will be transformed into frequency domain afterwards. Finally, the obtained iris image is cropped into an image of size 30 x 150.

3.2 Phase 2: Feature Extraction

The main objective of this step is extracting the feature of iris which will be used in classification step. This step consist of smoothing the iris pattern using window function, the transformation of iris pattern from spatial domain into frequency domain using Fast Fourier transform algorithm, and size reduction using Singular Value Decomposition.

3.2.1 Smoothing the Image

The main objective of applying window function is to smooth the signal. Hanning window function is considered to smooth the iris image. Window function length 15 is applied to normalize iris image which obtained from previous step, and multiply to the window of normalized image size 1 x 15 continuously from the top left position until bottom right. Hamming window function is described as equation (13).

$$w(n) = 0.5 \left(1 - \cos \left(2\pi \frac{n}{N} \right) \right), 0 \leq n \leq N \quad (13)$$

From the equation above, this would generate n point of coefficients where N is length of defined window, and then calculate the sum of product at any pixel of the iris image by sliding the window all over the image. This could reduce the spectral leakage of signal in the interested duration while analyzing.

3.2.2 Fast Fourier Transform

Fast Fourier Transform (FFT) algorithm is an efficient algorithm to compute the DFT (Discrete Fourier Transform). This operation is useful in many fields, especially in signal analysis. The merit of the FFT is its time consumption. In this step, the normalized image matrix from previous step is separated into each window of size 1 x 15 equally so there are 300 windows totally for each iris image. Then, Discrete Fourier Coefficients for each window are calculated by the following equation.

$$X(k) = \sum_{j=1}^N x(j) \omega_N^{(j-1)(k-1)} \quad (14)$$

And
$$\omega_N = e^{(2\pi i)/N}$$

Where

- $x(j)$ is intensity at pixel j of a considered window,
- N is window length, which is defined as 15 in this experiment.

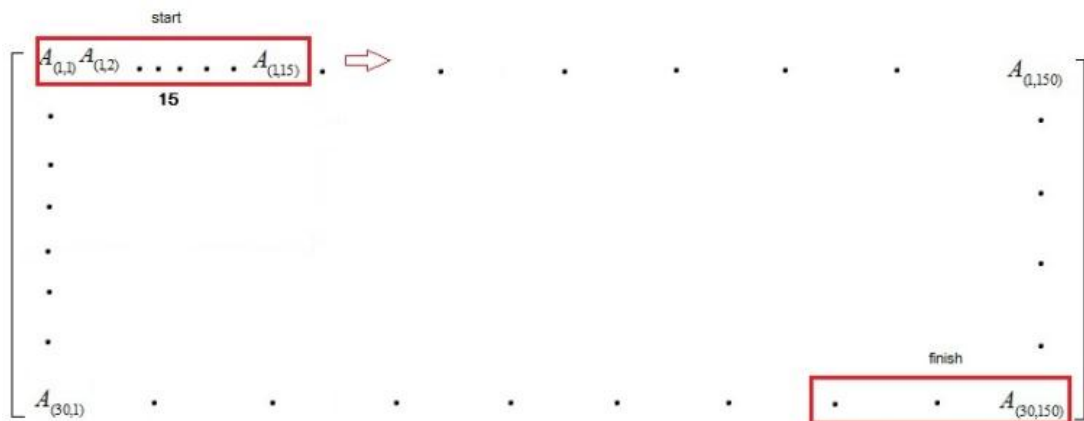


Figure 3.7a: Image is divided to small blocks of size 1 x 15.

Set of 15 Discrete Fourier coefficients is obtained for each window as shown in Figure 3.7a. Since there are ten windows for each row and 30 rows for an image, after this process, the number of coefficients for the iris image is $15 \times 10 \times 30 = 4500$, which is equal to the number of pixels of the normalized image.

Size of each coefficient window should not be too long or too short. Otherwise, this would directly affect performance of classification step. In this research, various sizes of the window were tested during Fourier transform. Length of 15 is most suitable among various sizes in terms of recognition performance because this length can achieve the local features of iris image. Figure 5 has shown the DFT computation from the start point until the finish point.

The plot of iris signal at a specific intervals after applying window function in equal length of 15 is depicted in Figure 6 where Y-axis denotes the pixel intensity of each point ranging from 0 to 1. Then; the sample signal is transformed into frequency domain which includes its amplitude of frequency coefficients against frequency as shown in Figure 3.8a and Figure 3.8b.

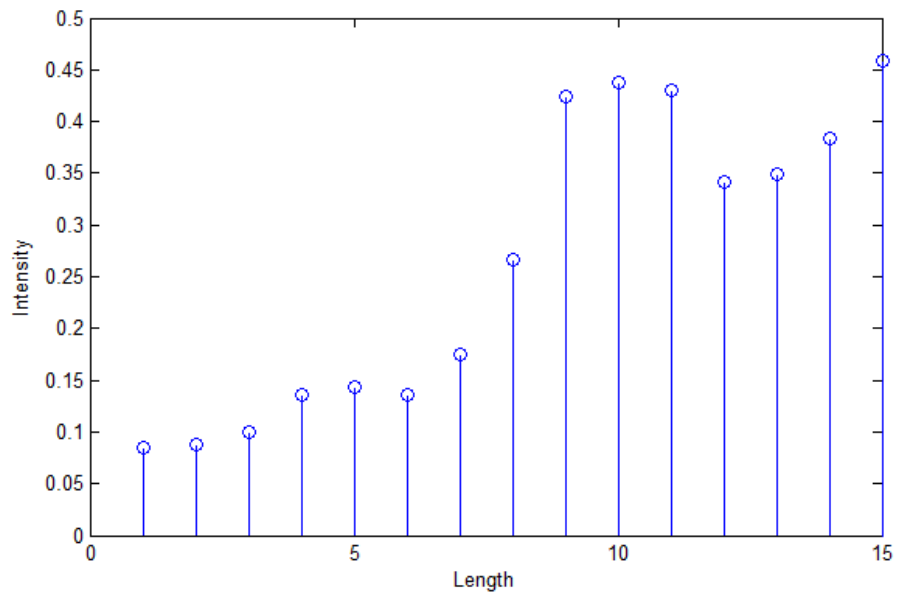


Figure 3.8a: Iris signal sample in spatial domain

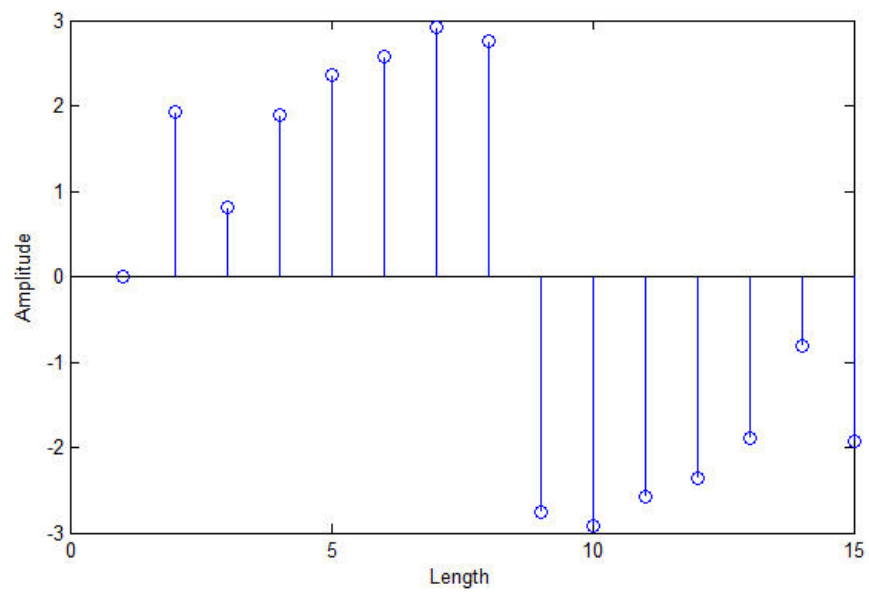
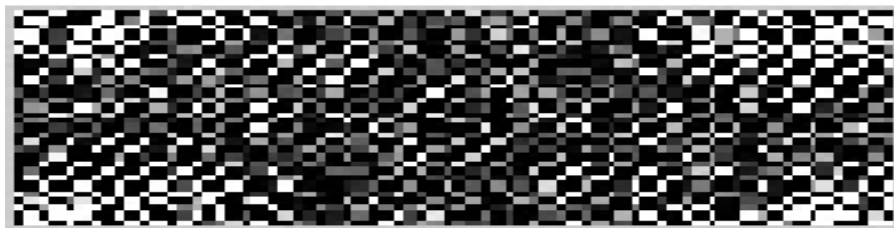


Figure 3.8b: Iris signal sample in frequency domain



(a)



(b)

Figure 3.9a: Normalized iris with preparing to apply Fast Fourier Transform Algorithm (a)
Before applying Fast Fourier Transform algorithm (b) After applying Fast Fourier
Transform algorithm

3.2.3 Singular Value Decomposition

After the transformation iris to frequency domain, iris frequency matrix is obtained. Iris's frequency matrix is separated into 15 x 15 block equally, then the SVD is applied with each block to produce the diagonal matrix with size is the same as that of frequency matrix. The computation starts from the upper left position until lower right position, which is the last block as shown in Figure 3.10a. In this experiment, both M and N for each block are 15.

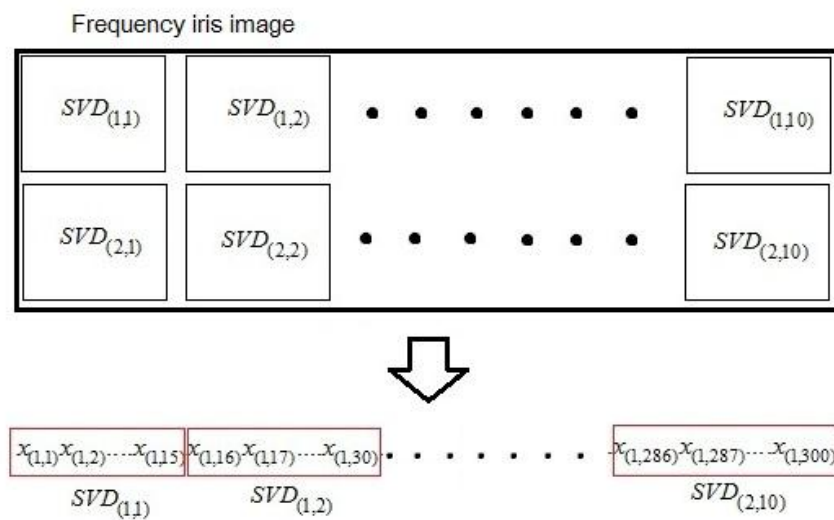


Figure 3.10a: Applying SVD to frequency matrix

Only main diagonal value of the matrix is considered because other elements are zero. This can automatically reduce size of each frequency block without significant loss of each frequency block. The results a single vector of size 15 for each block. The reason of dividing a frequency matrix into small blocks is to retain the significant local information of each frequency block. There are 20 frequency blocks after division step, and each block has its individual characteristic according to the iris pattern in that area. Since there are 20 frequency blocks each of which correspond to 15 features, number of feature is finally 300 for each iris image. When the feature extraction step was done, the classification step is provided to identify iris images.

3.3 Phase 3: Classification

3.3.1 Back Propagation Neural Network

Back Propagation Neural Network is adopted as a classification model. The back-propagation network is widely used in classification for adjusting the optimal weight of each node. Normal architecture of the network consists of one input layer, some hidden layers and one output layer. Every layer consists of an amount number of neurons, the number of connections between neurons, their corresponding weights and a threshold.

For this research, network architecture contains three layers: one input layer, one hidden layer, and one output layer. There are 300 features, fed into the input layer while the number of classes corresponding the number of individuals in the database. Figure 3.12a shows our network architecture.

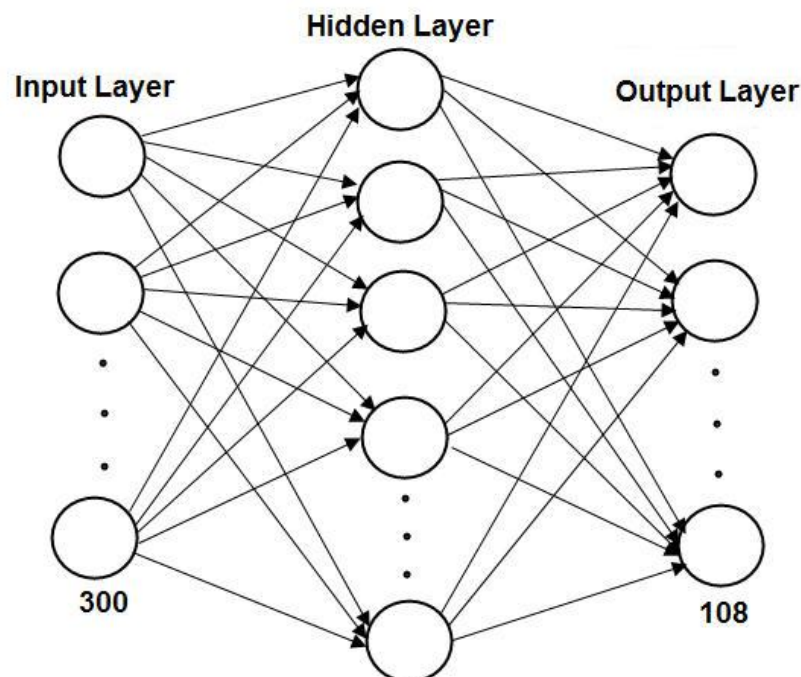


Figure 3.11a: Back Propagation network architecture

The concept of gradient descent and adaptive learning rate based on back propagation algorithm is used as training function of neural network. The advantage of this function is that the training process is accelerating converged by adjusting learning rate according to error change.

The weight updating is described in equation (15)

$$w^{k+1} = w^k - \eta g(w^k) \quad (15)$$

Where

- w^k is current iteration k
- η is learning rate
- $g(w)$ is the gradient vector calculated by applying chain rule on the layer

The activation function of our experiment is hyperbolic tangent sigmoid. This function is a kind of bipolar function whose output is ranging from -1 to 1. The function is used after the calculation at each output neuron in order to identify output class within the appropriate range. The function is calculated by

$$\tan(n) = \frac{2}{1 + e^{-2n}} - 1 \quad (16)$$

where n is a value computed from each neuron in output layer.

In this research, training process is performed in supervised mode. Initial learning rate parameter was set as 0.01 and momentum was set as 0.9 in order to increase the training efficiency. The target value was set as $[-1, 1]$ and the threshold was set at 0. Hence, after the classification, the element of target value which less than 0 is rejected from the class, otherwise, it is accepted.

CHAPTER IV

EXPERIMENTAL RESULT

This chapter describes the experimental result of research consist of two sections. The first section explains result of accuracy rate in iris identification system using Fast Fourier transform algorithm to extract feature and size reduction using Singular value decomposition.

In order to evaluate our method, the method is compared to typical methods on the same dataset named CASIA. In this dataset, the iris image is represented in gray scale, each of which size is 320*240. The total amount of class is 108 classes, each of which contains seven images.

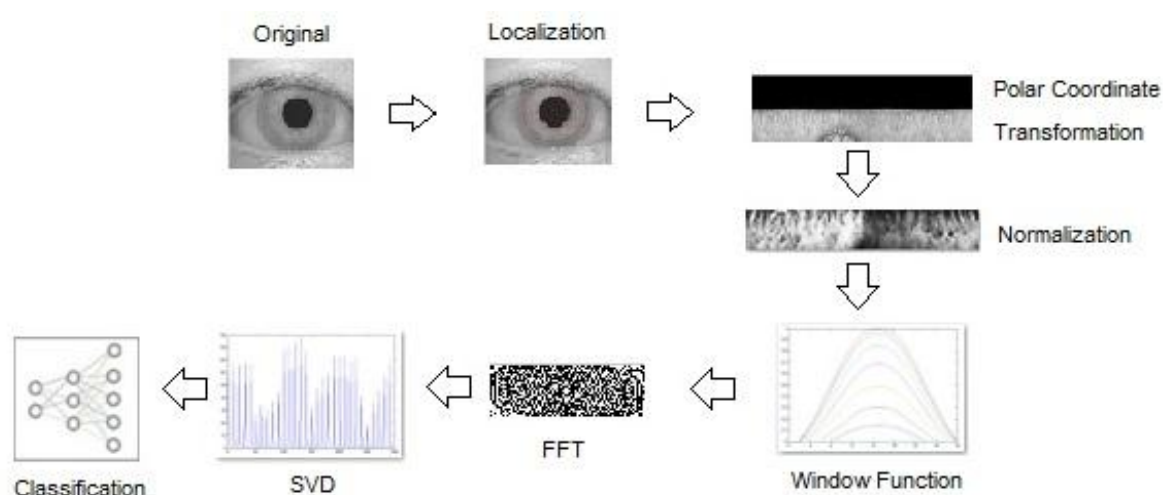


Figure 4.1a: Process summarization

Figure 4.1a shows the process summarization of this research. The first step, iris region is localized from the original image using Circular Hough Transform. After that, pupil radius, iris radius and center coordinate, which were derived from Circular Hough transform are used in Polar Coordinate Transformation in order to reform to rectangular iris image. In the next step, such rectangular image is normalized for eliminating unnecessary regions and balancing its pixel intensity. In order to smooth the image, window function is then applied to normalized image. The smoothed image is then transformed to frequency domain using FFT algorithm. After that, the frequency

matrix size is reduced to be feature vector using Singular Value Decomposition. Finally, the derived feature vector is fed into feed forward neural network as an input for classification.

4.1 The Experimental Result of Iris Identification

For this research, the result is obtained from experiment with iris database name CASIA [13]. The database consists of eye image from 108 people. The eye image resolution is represented in gray scale image size 320x240. Each person has 7 different images. The image is divided into 2 set. First is training set consist of 5 images per person. Second is test set consist of 2 image per person, so the ration of training set and test set is 5:2 respectively. The target value was set as $[-1, 1]$ and the threshold was set at 0. Hence, after the classification, the element of target value which is less than 0 is rejected from the class. Otherwise, it is accepted.

	A	B	C	D	E	F	G	H	I	J
1	0.978839	0.880262	-0.99978	-0.99991	-0.9958	-0.9988	-0.99906	-0.99951	-0.99807	-0.99969
2	-0.99994	-0.99998	0.974794	0.983463	-0.99822	-0.9986	-0.99888	-0.99992	-0.99974	-0.99986
3	-0.99986	-0.99999	-0.99999	-0.99998	0.975415	0.979103	-0.99954	-0.99989	-0.99831	-0.99729
4	-0.99976	-1	-0.99995	-0.99857	-0.99558	-0.99906	0.976789	0.973127	-0.99999	-0.99998
5	-0.99984	-0.99994	-0.99999	-0.99998	-0.99402	-0.99311	-0.99986	-0.99995	0.967998	0.830765

Figure 4.2a: Example of confusion matrix

Figure 4.2a demonstrates the confusion matrix of 5 persons, the value in matrix denotes the target value which is between $[-1, 1]$. The column denotes the order of test image, and each row denotes the class of classification. The value which higher than a threshold value (-1) will be accepted in that class. For example, for column A and B, the values are 0.978839 and 0.880262 corresponding to the first row. Hence, image A and B is accepted in the first class in classification.

Figure 4.2b - Figure 4.2j are plot of classification result with various amount of neural node in hidden layer. The best classification result is using 250 neural nodes in hidden layer which is around 93.98%

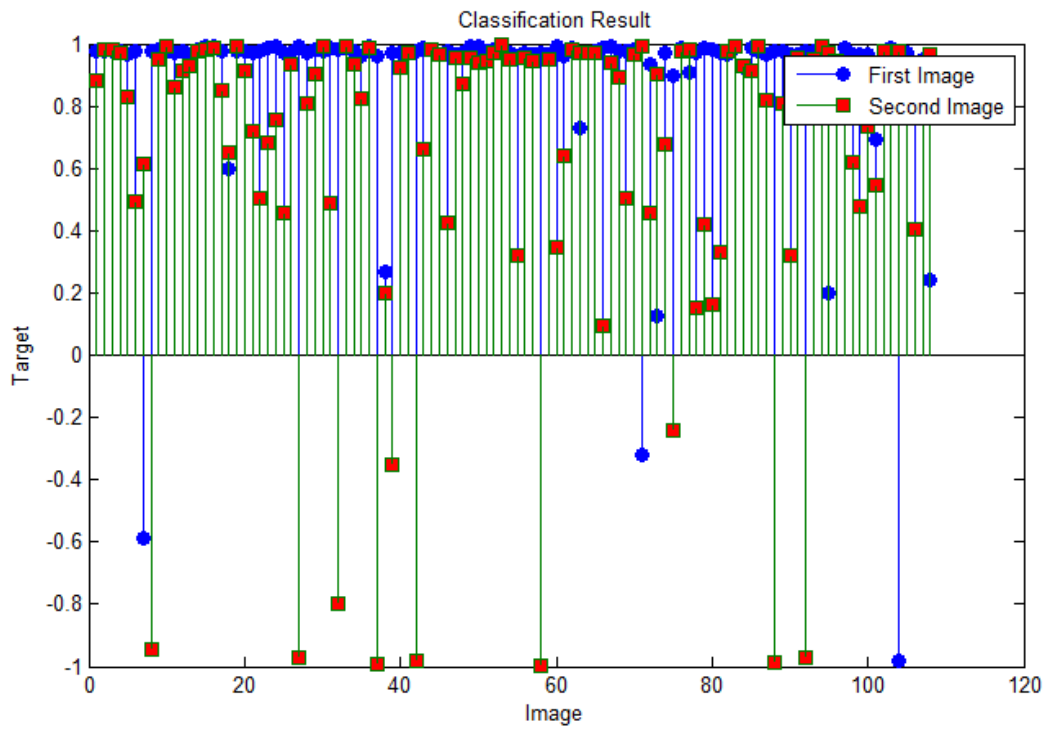


Figure 4.2b: Plot of classification result with 250 nodes in hidden layer

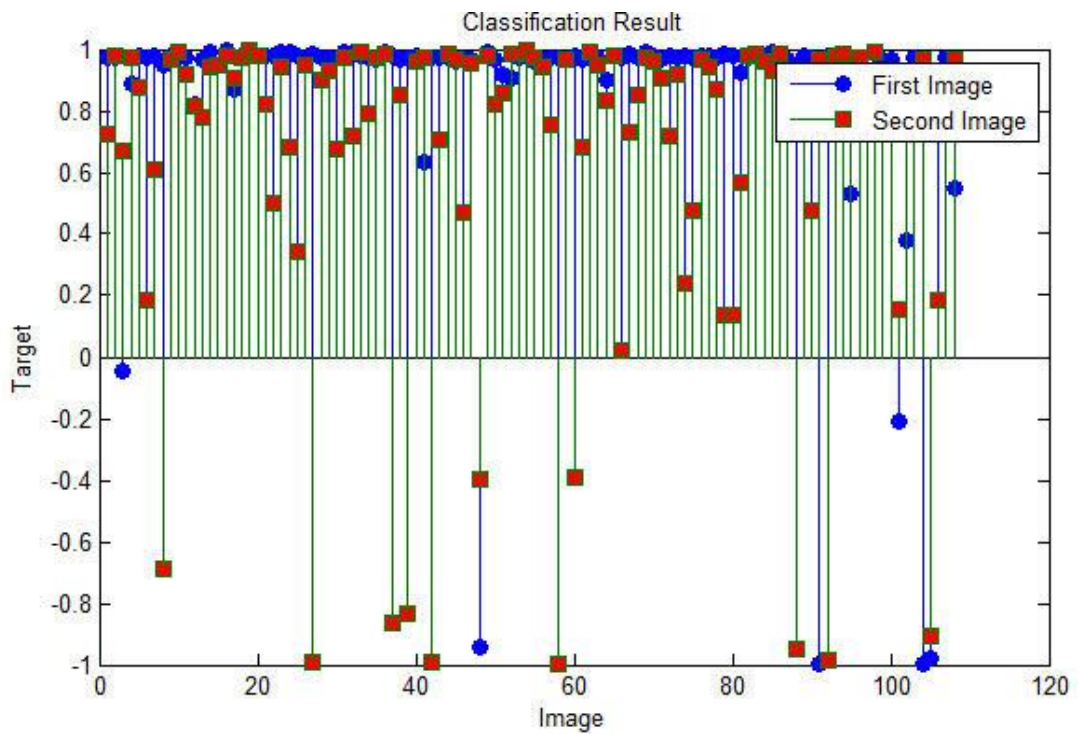


Figure 4.2c: Plot of classification result with 230 nodes in hidden layer

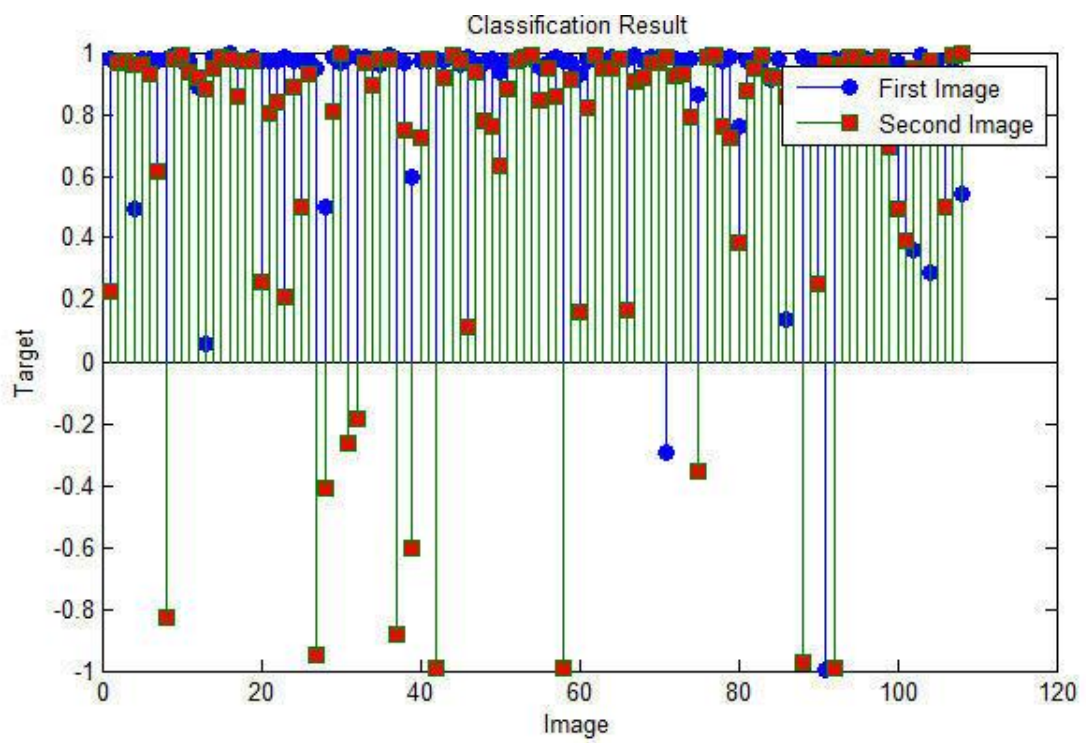


Figure 4.2d: Plot of classification result with 210 nodes in hidden layer

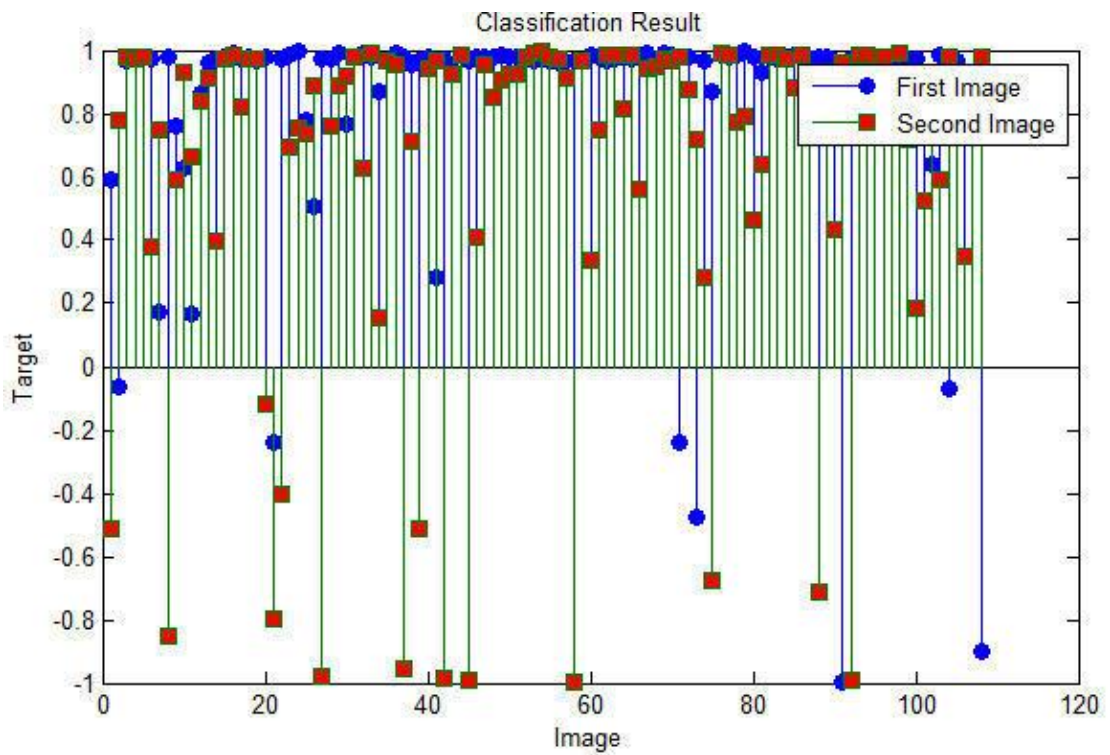


Figure 4.2e: Plot of classification result with 190 nodes in hidden layer

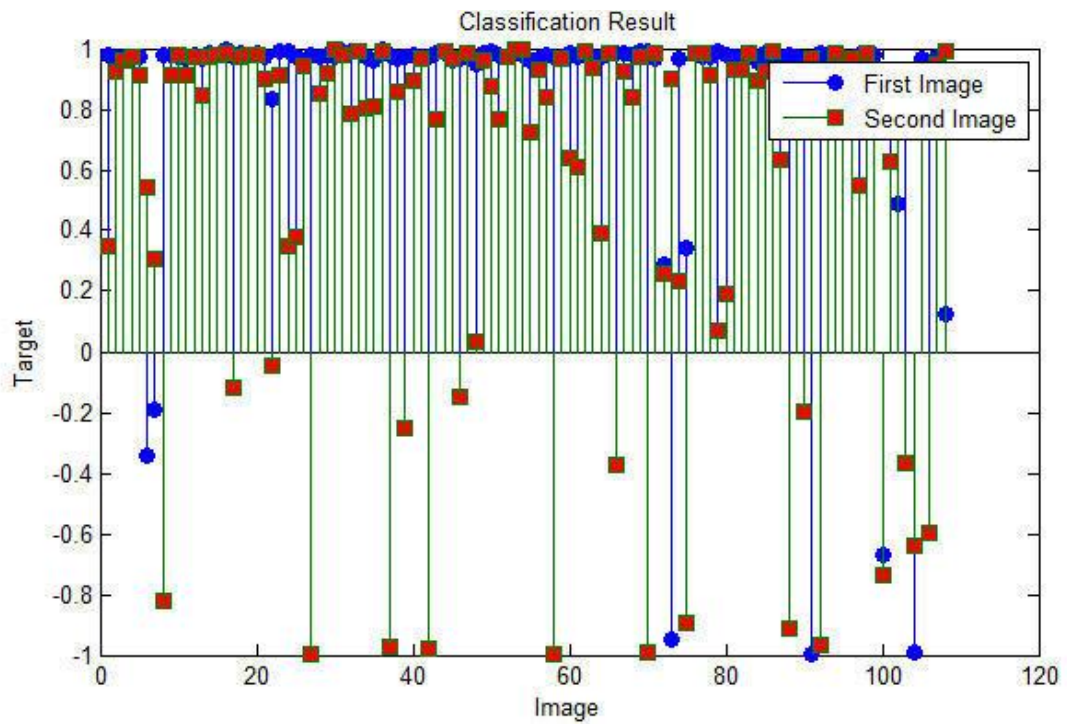


Figure 4.2f: Plot of classification result with 170 nodes in hidden layer

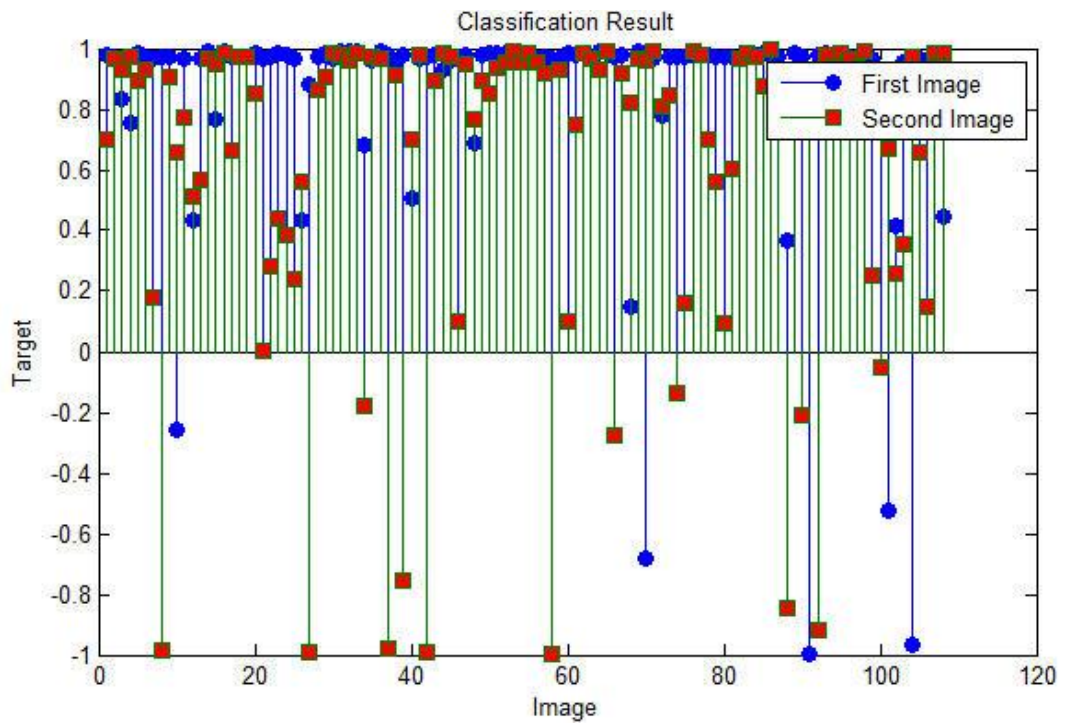


Figure 4.2g: Plot of classification result with 150 nodes in hidden layer

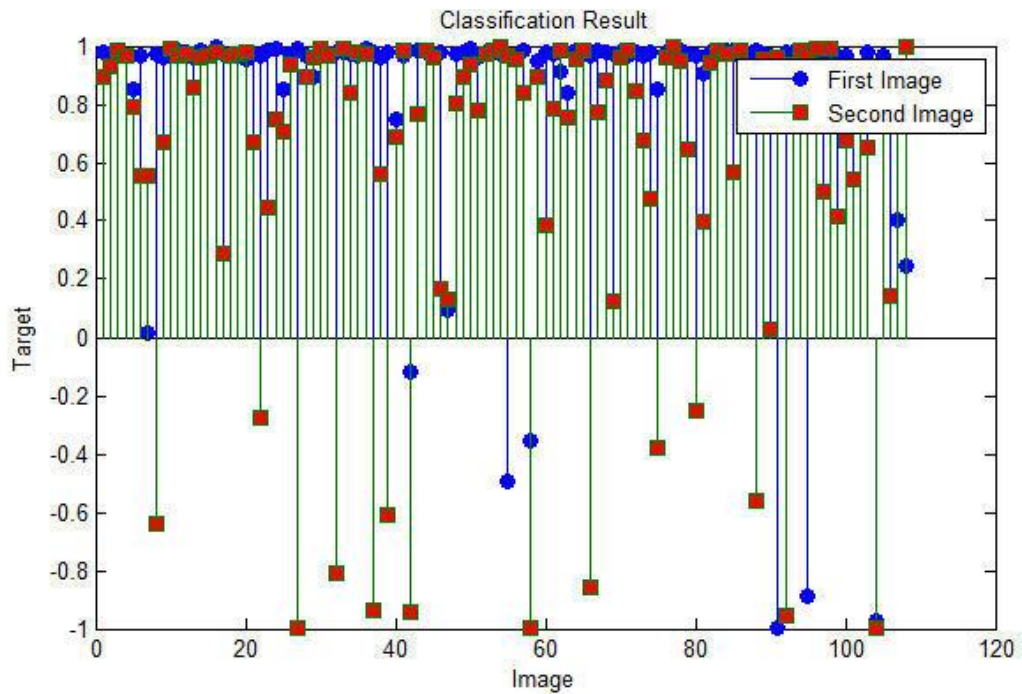


Figure 4.2h: Plot of classification result with 130 nodes in hidden layer

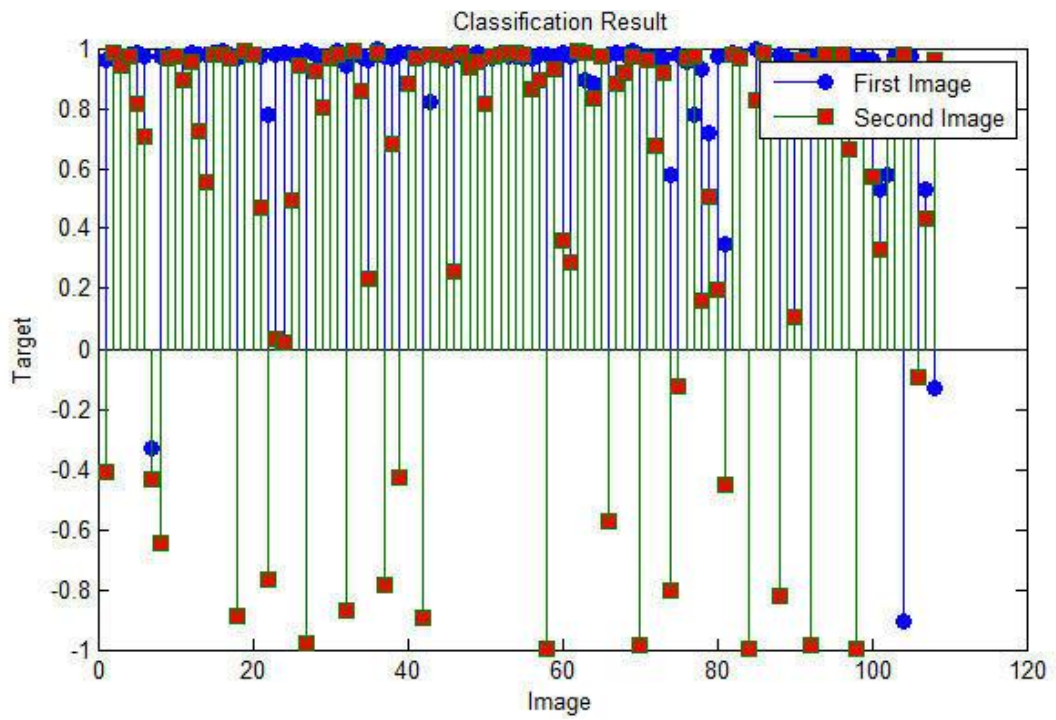


Figure 4.2i: Plot of classification result with 110 nodes in hidden layer

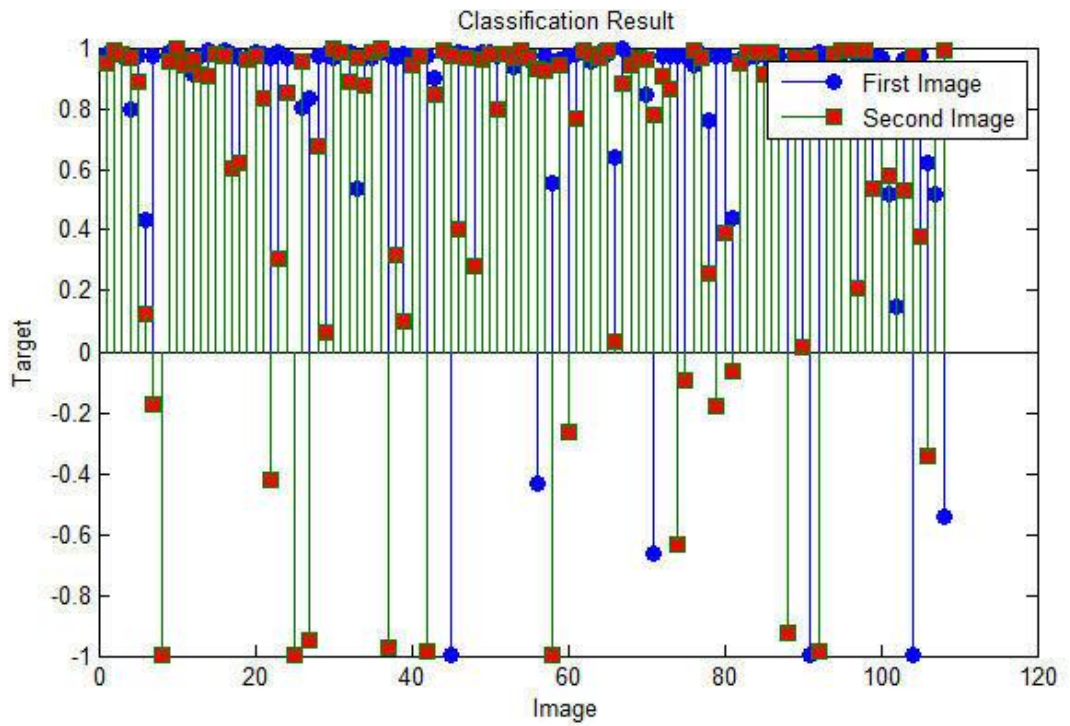


Figure 4.2j: Plot of classification result with 90 nodes in hidden layer

Table 4.1 Demonstrate the result of classification. The column Value is the value computed by neural network range between -1 and 1. There are two images used as test data of this research. The overall accuracy can be computed as following equation.

$$\text{Accuracy}\% = \frac{\text{Number of correct classification}}{\text{Total of testing image}} \quad (17)$$

From this experiment, amount of total test image are 216 and the collect classification are 203, so the accuracy of identification is 93.98%

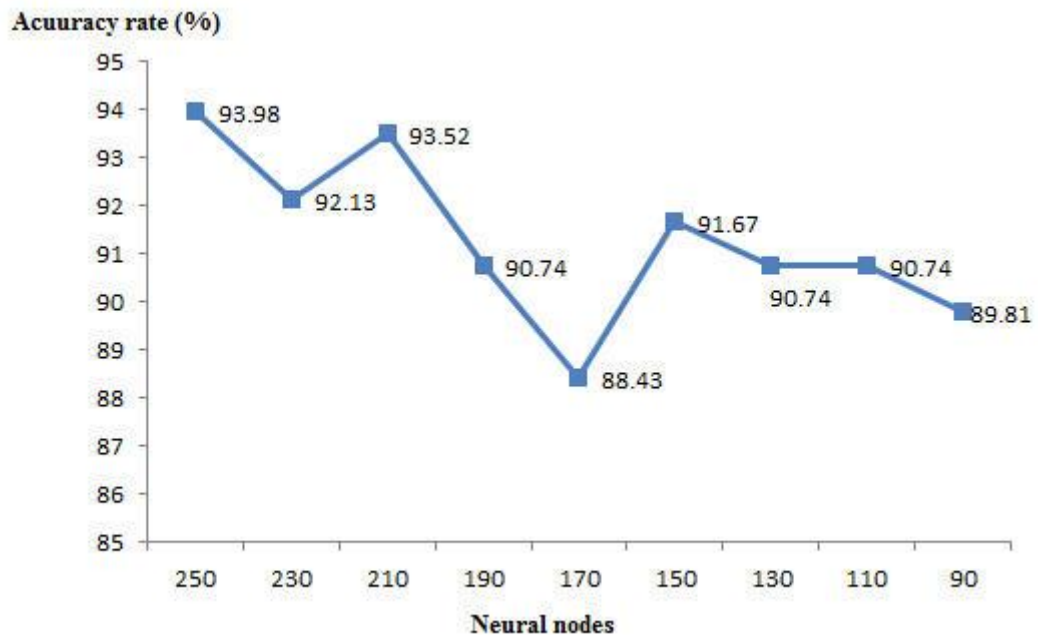


Figure 4.3a: Plot of classification result with amount of neurals in hidden layer

Person	1st Image			2nd Image		
	Value	Accept	Reject	Value	Accept	Reject
1	0.9788391	✓		0.880262	✓	
2	0.9747941	✓		0.983463	✓	
3	0.9754148	✓		0.979103	✓	
4	0.9767891	✓		0.973127	✓	
5	0.9679985	✓		0.830765	✓	

Person	1st Image			2nd Image		
	Value	Accept	Reject	Value	Accept	Reject
6	0.9770954	✓		0.490923	✓	
7	-0.587951		✘	0.612657	✓	
8	0.9765065	✓		-0.94504		✘
9	0.9818401	✓		0.95046	✓	
10	0.9764585	✓		0.990328	✓	
11	0.9699066	✓		0.863	✓	
12	0.9738882	✓		0.91235	✓	
13	0.9656423	✓		0.930947	✓	
14	0.9810018	✓		0.975412	✓	
15	0.9917327	✓		0.98294	✓	
16	0.9946859	✓		0.986361	✓	
17	0.97516	✓		0.849724	✓	
18	0.5992533	✓		0.648845	✓	
19	0.9772138	✓		0.992237	✓	
20	0.9768651	✓		0.911261	✓	
21	0.9729557	✓		0.719132	✓	
22	0.974991	✓		0.503597	✓	
23	0.9873632	✓		0.684036	✓	
24	0.9939955	✓		0.758226	✓	
25	0.9726816	✓		0.455726	✓	
26	0.9718515	✓		0.932896	✓	
27	0.9901202	✓		-0.97229		✘
28	0.9712584	✓		0.809812	✓	
29	0.9791281	✓		0.90284	✓	
30	0.9773181	✓		0.991585	✓	
31	0.986585	✓		0.487307	✓	
32	0.983477	✓		-0.79956		✘

Person	1st Image			2nd Image		
	Value	Accept	Reject	Value	Accept	Reject
33	0.9868513	✓		0.989788	✓	
34	0.9756131	✓		0.935338	✓	
35	0.9592644	✓		0.825357	✓	
36	0.9946823	✓		0.988546	✓	
37	0.9602656	✓		-0.99242		x
38	0.2693766	✓		0.198398	✓	
39	0.9736738	✓		-0.3543		x
40	0.9728472	✓		0.924002	✓	
41	0.9731576	✓		0.970707	✓	
42	0.974068	✓		-0.98258		x
43	0.9872506	✓		0.662042	✓	
44	0.9819542	✓		0.983575	✓	
45	0.9648735	✓		0.96715	✓	
46	0.9777487	✓		0.425241	✓	
47	0.9664223	✓		0.95287	✓	
48	0.9714292	✓		0.872003	✓	
49	0.992467	✓		0.957834	✓	
50	0.9907004	✓		0.941087	✓	
51	0.9766217	✓		0.945829	✓	
52	0.9832324	✓		0.969997	✓	
53	0.9865476	✓		0.995489	✓	
54	0.9713038	✓		0.950549	✓	
55	0.9583974	✓		0.321483	✓	
56	0.97188	✓		0.955414	✓	
57	0.9661293	✓		0.943564	✓	
58	0.9686299	✓		-0.99504		x
59	0.9658249	✓		0.949415	✓	

Person	1st Image			2nd Image		
	Value	Accept	Reject	Value	Accept	Reject
60	0.9902362	✓		0.344861	✓	
61	0.9611366	✓		0.641818	✓	
62	0.9855032	✓		0.982427	✓	
63	0.7295619	✓		0.973747	✓	
64	0.9694344	✓		0.969581	✓	
65	0.9786265	✓		0.972281	✓	
66	0.9848824	✓		0.094434	✓	
67	0.9933907	✓		0.938895	✓	
68	0.9761016	✓		0.890998	✓	
69	0.9754838	✓		0.503199	✓	
70	0.9807567	✓		0.966185	✓	
71	-0.320114		x	0.994341	✓	
72	0.9351995	✓		0.458854	✓	
73	0.1276369	✓		0.900522	✓	
74	0.9727196	✓		0.675955	✓	
75	0.8996676	✓		-0.24382		x
76	0.9875195	✓		0.977489	✓	
77	0.9100174	✓		0.980131	✓	
78	0.9725427	✓		0.154648	✓	
79	0.9871545	✓		0.422469	✓	
80	0.981262	✓		0.162991	✓	
81	0.9702325	✓		0.332587	✓	
82	0.9667858	✓		0.976251	✓	
83	0.9854932	✓		0.991278	✓	
84	0.9215432	✓		0.928789	✓	
85	0.9883357	✓		0.913011	✓	
86	0.9765486	✓		0.99046	✓	

Person	1st Image			2nd Image		
	Value	Accept	Reject	Value	Accept	Reject
87	0.9664986	✓		0.821085	✓	
88	0.9753594	✓		-0.98895		✘
89	0.9739197	✓		0.80801	✓	
90	0.965993	✓		0.318701	✓	
91	0.9653243	✓		0.955698	✓	
92	0.9737887	✓		-0.96936		✘
93	0.9770102	✓		0.949673	✓	
94	0.9616138	✓		0.994348	✓	
95	0.1981051	✓		0.971007	✓	
96	0.9191497	✓		0.945764	✓	
97	0.986183	✓		0.818792	✓	
98	0.9646857	✓		0.618023	✓	
99	0.9678275	✓		0.479918	✓	
100	0.9676917	✓		0.732325	✓	
101	0.6945468	✓		0.543335	✓	
102	0.8315687	✓		0.974638	✓	
103	0.9855836	✓		0.86211	✓	
104	-0.981261		✘	0.973791	✓	
105	0.971333	✓		0.936281	✓	
106	0.9350984	✓		0.405432	✓	
107	0.9519883	✓		0.900395	✓	
108	0.2430047	✓		0.966708	✓	

Table 4.1: Experimental result of test image with the system

4.2 Discussion

Daugman's method performs the best in terms of recognition rate. Two-dimensional iris data is transformed into iris code, and then Hamming distance is used as the dissimilarity measure between them. The result of this method gives very high accuracy of recognition rate. In contrast, size of feature is very large. This could be the problem in practically used in some environment which has limitation in space.

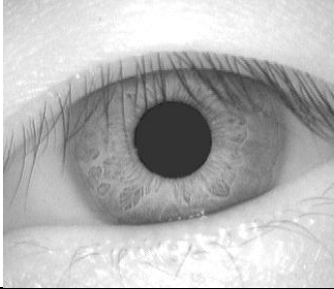
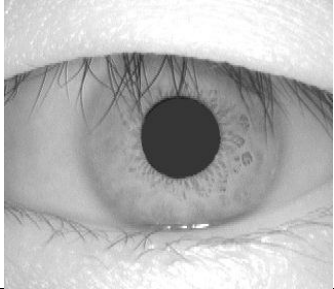
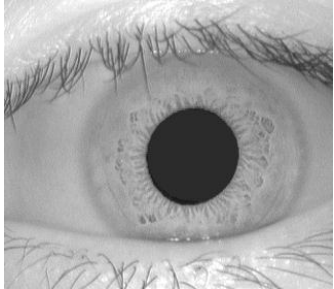
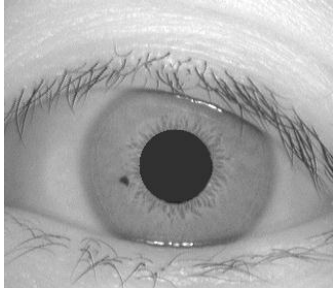
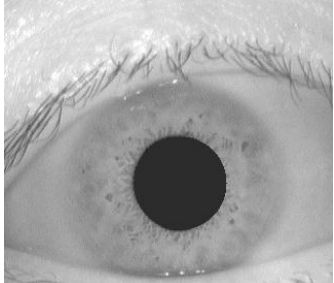
Kekre's method mainly focuses on small feature and time consuming which can reduce in space complexity and the overall process. The obvious advantage of this method is size of feature. Their feature size is just 16x12 when compared with other techniques. Moreover, a preprocessing step is not required in their feature extraction process. The drawback of this method is the accuracy rate is drop down to 81.25% - 89.10%.

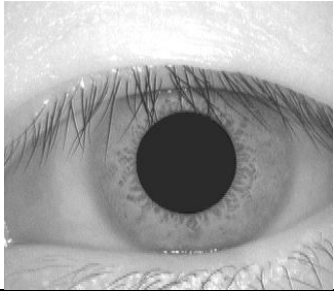
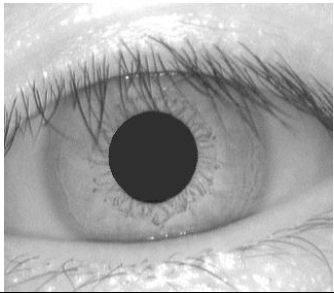
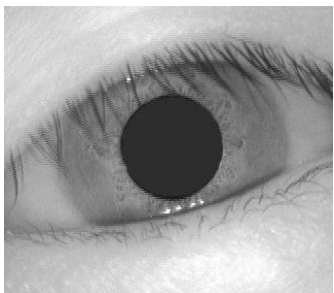
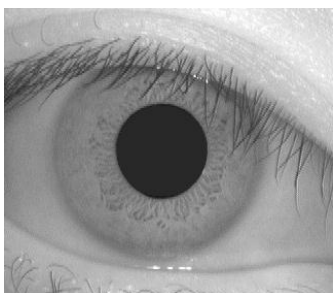
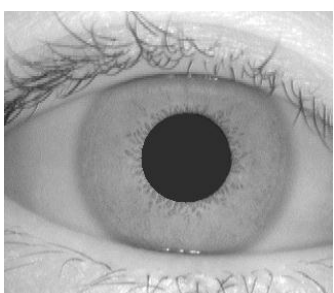
Boles's method adopts only the interest region around the pupil. This method emphasizes on size reduction of feature. According to its small size feature, computation time will be decreased as well. In contrast, only particular circle region around the pupil is not significant enough. The drawback of this method is the dropping of accuracy rate 92.64%

Method	Size of feature	Accuracy
Daugman	2048	100%
Bole	256	92.64%
Kekre	192	89.10%
Proposed	300	93.98

Table 4.2: Comparison with other technique

However, the proposed technique still has some limitation. The misclassifications of this work are occurring from blurred image and the interference of noisy data. The following is the example of misclassification image:

Person/Image	Image	Value	Noisy data	Blurred
7/2		-0.587951	✓	
8/2		-0.94504	✓	
27/2		-0.97229		✓
32/2		-0.79956	✓	
37/2		-0.99242		✓

Person/Image	Image	Value	Noisy data	Blurred
39/2		-0.3543	✓	
42/2		-0.98258	✓	
58/2		-0.99504	✓	
71/1		-0.320114	✓	
75/2		-0.24382		✓

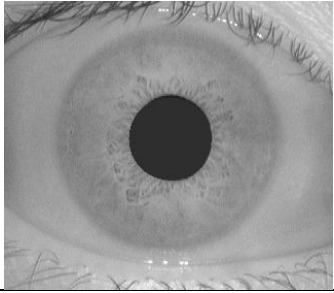
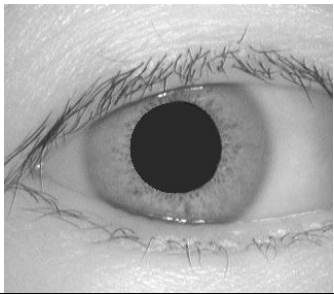
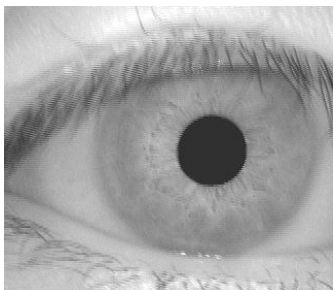
Person/Image	Image	Value	Noisy data	Blurred
88/2		-0.98895		✓
92/2		-0.96936	✓	
104/1		-0.981261		✓

Table 4.3: Demonstration of misclassification image

The misclassification mostly occurs with the low quality image. In this research, the error causes from two main problems which are blurred image and noisy image. Table 4.3 demonstrates the misclassification image causing from two cases. The blurred image directly affects to the classification unclear iris texture. Another case is the noisy iris image, the noise data in both eyelid and eyelash both will superimpose the iris texture while feature is extracted. This research mainly relies on the frequency of iris texture. In the future, this research will be improved to handle with the low-quality eye image.

CHAPTER V

CONCLUSION

This research proposed new iris identification based on Fourier Coefficient and Singular Value Decomposition. The main idea is to transform the extracted iris pattern from spatial domain into frequency domain and then reduce size of frequency matrix by applying Singular Value Decomposition. Size of each feature is 300 which is smaller than other technique. The main objective is to reduce the space complexity in iris data collection to collect the feature in practically used while the accuracy rate of identification is in the acceptable level. However, some limitation of this system still remains. The classification errors occur from blurred and noisy image.

The strength points of this research are using small size of feature while compared with other technique, and the accuracy rate is in acceptable level. In the future, this research will be improved in time consuming of overall process from localization step to classification step, and the method to handle with the low-quality image is also improved.

REFERENCE

- [1] H. B. Kekre, T. K. Sarode, and V. A. Bharadi, "Iris Recognition using Vector Quantization." International Conference on Signal Acquisition and Processing, pp.: 217–218 Feb. 2010.
- [2] Jim Z.C. Lai, Yi-Ching Liaw, and Julie Liu, "A fast VQ Codebook Generation Algorithm using Codeword Displacement", Pattern Recognition vol. 41, no. 1, pp.: 315–319, 2008.
- [3] C.C. Chang, Wen-Chuan Wu, "Fast Planar-Oriented Ripple Search Algorithm for Hyperspace VQ Codebook", IEEE Transactions on image processing, vol 16, no. 6, pp.: 1538-1547, June 2007.
- [4] Y. Linde, A. Buzo, and R. M. Gray, "An Algorithm for Vector Quantizer Design." IEEE Transactions Communication, vol. COM-28, no. 1, pp.: 84-95, 1980.
- [5] W. W. Boles, B. Boashash, "A Human Identification Technique using Images of the Iris and Wavelet Transform." IEEE Transactions on Signal Processing, vol. 46, no. 4, pp. 1185–1188, 1998.
- [6] J. Daugman, "Statistical Richness of Visual Phase Information: update on recognizing persons by iris patterns." International Journal of Computer Vision, vol. 45, no. 1, pp. 25–38, 2001.
- [7] C. Kimme, D. Ballard, J. Sklansky, "Finding Circles by an Array of Accumulator.", Proceeding ACM, Vol.18, no.2, pp. 120-122, Feb. 1975.
- [8] Brown, Richard G. Andrew M. Gleason," Advanced Mathematics: Precalculus with Discrete Mathematics and Data Analysis. Evanston", Illinois: McDougal Littell. 1997.
- [9] GA Korn, TM Korn, "Mathematical Handbook for Scientists and Engineers", New York: McGraw-Hill, 1961.
- [10] Brenner, N.; C. Rader, "A New Principle for Fast Fourier Transformation". IEEE Acoustics, Speech & Signal Processing 24 (3): 264–266, 1976.

- [11] Horn, Roger A.; Johnson, Charles R. "Matrix Analysis", Cambridge University Press, 1985.
- [12] J. J. HOPFIELD, "Neural Networks and Physical Systems with Emergent Collective Computational Abilities", Proceeding Nat L Acad. Science USA Vol. 79, pp. 2554-2558, April 1982.
- [13] Iris Image Database- Iris Recognition Research Group National Laboratory of Pattern Recognition (NLPR) Institute of Automation, Chinese Academy of Sciences, <http://www.sinobiometrics.com>.

APPENDIX

APPENDIX: Illustration of the classification result of training set.

1. The classification result of training set for 1st and 2nd image.

Person	1st Image			2nd Image		
	Value	Accept	Reject	Value	Accept	Reject
1	0.961568	✓		0.993916	✓	
2	0.969371	✓		0.975382	✓	
3	0.978582	✓		0.975361	✓	
4	0.984704	✓		0.979003	✓	
5	0.98426	✓		0.965819	✓	
6	0.970703	✓		0.951483	✓	
7	0.966784	✓		0.989156	✓	
8	0.981033	✓		0.979074	✓	
9	0.965924	✓		0.969189	✓	
10	0.956068	✓		0.53428	✓	
11	0.982993	✓		0.973084	✓	
12	0.963323	✓		0.813802	✓	
13	0.973614	✓		0.973856	✓	
14	0.983321	✓		0.973132	✓	
15	-0.77856		✗	0.356421	✓	
16	-0.74129		✗	0.114518	✓	
17	0.974792	✓		0.978172	✓	
18	0.977354	✓		0.967233	✓	
19	0.982869	✓		0.939351	✓	
20	0.986353	✓		0.971436	✓	
21	0.992118	✓		0.972096	✓	
22	0.986357	✓		0.987864	✓	
23	0.973944	✓		0.98151	✓	
24	0.953708	✓		0.936486	✓	
25	0.996692	✓		0.976617	✓	

Person	1st Image			2nd Image		
	Value	Accept	Reject	Value	Accept	Reject
26	0.980314	✓		0.982485	✓	
27	0.967392	✓		0.981988	✓	
28	0.971657	✓		0.988873	✓	
29	0.814524	✓		0.97966	✓	
30	-0.85662		x	0.97623	✓	
31	0.92827	✓		0.969423	✓	
32	0.989797	✓		0.972339	✓	
33	0.974831	✓		0.991622	✓	
34	0.993342	✓		0.977228	✓	
35	0.979372	✓		0.98053	✓	
36	0.958894	✓		0.979163	✓	
37	0.975981	✓		0.741327	✓	
38	0.972192	✓		0.978445	✓	
39	0.980542	✓		0.977776	✓	
40	0.994307	✓		0.989833	✓	
41	0.980085	✓		0.980085	✓	
42	0.982492	✓		0.982935	✓	
43	0.942793	✓		0.968752	✓	
44	0.993588	✓		0.948221	✓	
45	0.833692	✓		0.973696	✓	
46	0.981883	✓		0.987187	✓	
47	0.968124	✓		0.987371	✓	
48	0.974209	✓		0.982846	✓	
49	0.96959	✓		0.97898	✓	
50	0.37537	✓		0.987797	✓	
51	0.971777	✓		0.97622	✓	
52	0.994852	✓		0.975005	✓	
53	0.970536	✓		0.978308	✓	

Person	1st Image			2nd Image		
	Value	Accept	Reject	Value	Accept	Reject
54	0.974374	✓		0.992469	✓	
55	0.988696	✓		0.979923	✓	
56	0.965935	✓		0.981146	✓	
57	0.973442	✓		0.971728	✓	
58	0.992622	✓		0.979932	✓	
59	0.986708	✓		0.965133	✓	
60	-0.00219		✘	0.97027	✓	
61	0.942858	✓		0.973436	✓	
62	0.980974	✓		0.977833	✓	
63	0.962124	✓		0.985819	✓	
64	0.96836	✓		0.717636	✓	
65	0.976288	✓		0.980921	✓	
66	0.97751	✓		0.984936	✓	
67	0.783052	✓		0.975492	✓	
68	0.97848	✓		0.815719	✓	
69	0.970915	✓		0.903818	✓	
70	0.983181	✓		0.973953	✓	
71	0.982482	✓		0.994042	✓	
72	0.989478	✓		0.976058	✓	
73	0.748666	✓		0.960929	✓	
74	0.972904	✓		0.981035	✓	
75	0.967858	✓		0.294901	✓	
76	0.992513	✓		0.983568	✓	
77	0.979592	✓		0.993089	✓	
78	0.71022	✓		0.973074	✓	
79	0.977249	✓		0.958453	✓	
80	0.977051	✓		0.9451	✓	
81	0.964833	✓		0.969643	✓	

Person	1st Image			2nd Image		
	Value	Accept	Reject	Value	Accept	Reject
82	0.748749	✓		0.977057	✓	
83	0.975974	✓		0.974476	✓	
84	0.979583	✓		0.982559	✓	
85	0.969616	✓		0.981632	✓	
86	0.982098	✓		0.977798	✓	
87	0.966023	✓		0.975956	✓	
88	0.977325	✓		0.993963	✓	
89	0.976899	✓		0.969054	✓	
90	0.987188	✓		0.966724	✓	
91	0.969318	✓		0.965252	✓	
92	0.963913	✓		0.896419	✓	
93	0.977142	✓		0.98279	✓	
94	0.971178	✓		0.971697	✓	
95	0.975244	✓		0.989214	✓	
96	0.988337	✓		0.984924	✓	
97	0.970967	✓		0.966047	✓	
98	0.980557	✓		0.967434	✓	
99	0.973322	✓		0.951519	✓	
100	0.970272	✓		-0.27826		x
101	0.984406	✓		0.977365	✓	
102	0.437581	✓		0.760504	✓	
103	0.979808	✓		0.973825	✓	
104	0.980341	✓		0.968828	✓	
105	0.983302	✓		0.939872	✓	
106	0.752628	✓		0.974961	✓	
107	0.972327	✓		0.974668	✓	
108	0.972608	✓		-0.99169		x

2. The classification result of training set for 3rd and 4th image.

Person	3rd Image			4th Image		
	Value	Accept	Reject	Value	Accept	Reject
1	0.96969	✓		0.980454	✓	
2	0.746556	✓		0.967044	✓	
3	0.986822	✓		0.976915	✓	
4	0.973871	✓		0.985156	✓	
5	0.970905	✓		0.981826	✓	
6	0.980267	✓		0.551317	✓	
7	0.96923	✓		0.987594	✓	
8	0.973518	✓		0.909983	✓	
9	0.995805	✓		0.981606	✓	
10	0.982814	✓		0.979944	✓	
11	0.97701	✓		0.936435	✓	
12	0.973479	✓		0.981667	✓	
13	0.983977	✓		0.9654	✓	
14	0.973484	✓		0.973635	✓	
15	0.99998	✓		-0.99999		✘
16	0.963671	✓		0.936255	✓	
17	0.987382	✓		0.971011	✓	
18	0.972559	✓		0.990677	✓	
19	0.969656	✓		0.467377	✓	
20	0.97791	✓		0.973097	✓	
21	0.979425	✓		0.991636	✓	
22	0.987079	✓		0.966498	✓	
23	0.992238	✓		0.978611	✓	
24	0.969943	✓		0.971863	✓	
25	0.981374	✓		0.983309	✓	
26	0.988437	✓		0.968285	✓	
27	0.984293	✓		0.490817	✓	

Person	3rd Image			4th Image		
	Value	Accept	Reject	Value	Accept	Reject
28	0.983728	✓		0.977641	✓	
29	0.962533	✓		0.98669	✓	
30	-0.99815		✘	0.964568	✓	
31	0.972534	✓		0.862352	✓	
32	0.985441	✓		0.971645	✓	
33	0.98412	✓		0.96876	✓	
34	0.993803	✓		0.965346	✓	
35	0.975494	✓		0.972686	✓	
36	0.979736	✓		0.97836	✓	
37	0.971761	✓		0.881217	✓	
38	0.898624	✓		0.971786	✓	
39	0.979779	✓		0.992045	✓	
40	0.993462	✓		0.97062	✓	
41	0.975724	✓		0.972953	✓	
42	0.969668	✓		0.979277	✓	
43	0.988632	✓		0.970345	✓	
44	0.977394	✓		0.972408	✓	
45	0.97272	✓		0.964341	✓	
46	0.97149	✓		0.991526	✓	
47	0.925717	✓		0.964218	✓	
48	0.987156	✓		0.995003	✓	
49	0.9703	✓		0.99077	✓	
50	0.961274	✓		0.968478	✓	
51	0.97622	✓		0.976615	✓	
52	0.917649	✓		0.969193	✓	
53	0.979189	✓		0.986974	✓	
54	0.991045	✓		0.976431	✓	
55	0.970633	✓		0.993527	✓	

Person	3rd Image			4th Image		
	Value	Accept	Reject	Value	Accept	Reject
56	0.989249	✓		0.913486	✓	
57	0.722603	✓		0.977967	✓	
58	0.98438	✓		0.987831	✓	
59	0.967968	✓		0.953961	✓	
60	0.978385	✓		0.981788	✓	
61	0.983936	✓		0.972458	✓	
62	0.984421	✓		0.804229	✓	
63	0.976535	✓		0.87604	✓	
64	0.968223	✓		0.756389	✓	
65	0.985184	✓		0.980001	✓	
66	0.979539	✓		0.971489	✓	
67	0.875454	✓		0.965999	✓	
68	0.969419	✓		0.98059	✓	
69	0.958365	✓		0.987329	✓	
70	0.971662	✓		0.964493	✓	
71	0.973791	✓		0.981863	✓	
72	0.991838	✓		0.969767	✓	
73	0.744682	✓		0.976215	✓	
74	0.975079	✓		0.974266	✓	
75	0.975296	✓		0.986561	✓	
76	0.9775	✓		0.96839	✓	
77	0.974544	✓		0.0586	✓	
78	0.986754	✓		0.960879	✓	
79	0.818895	✓		0.971005	✓	
80	0.980479	✓		0.981336	✓	
81	0.957714	✓		0.934819	✓	
82	0.981446	✓		0.989077	✓	
83	0.620428	✓		0.969299	✓	

Person	3rd Image			4th Image		
	Value	Accept	Reject	Value	Accept	Reject
84	0.964916	✓		0.988188	✓	
85	0.871256	✓		0.983252	✓	
86	0.990208	✓		0.976547	✓	
87	0.963278	✓		0.964488	✓	
88	0.978307	✓		0.97537	✓	
89	0.979008	✓		0.975376	✓	
90	0.981953	✓		0.971906	✓	
91	0.982877	✓		0.623432	✓	
92	0.921993	✓		0.974451	✓	
93	0.979781	✓		0.988039	✓	
94	0.992335	✓		0.959816	✓	
95	0.975456	✓		0.982892	✓	
96	0.978316	✓		0.985017	✓	
97	0.99285	✓		0.996538	✓	
98	0.971871	✓		0.973413	✓	
99	0.99806	✓		0.969177	✓	
100	0.978188	✓		0.984779	✓	
101	0.970598	✓		0.971399	✓	
102	0.978165	✓		0.969102	✓	
103	0.978665	✓		0.979426	✓	
104	0.978227	✓		0.962107	✓	
105	0.944176	✓		0.96504	✓	
106	0.928608	✓		0.969337	✓	
107	0.804682	✓		0.96646	✓	
108	0.980007	✓		0.978735	✓	

3. The classification result of training set for 5th image.

Person	5th Image		
	Value	Accept	Reject
1	0.97403	✓	
2	0.275931	✓	
3	0.972527	✓	
4	0.985156	✓	
5	0.890976	✓	
6	0.547792	✓	
7	0.97501	✓	
8	0.875174	✓	
9	0.975734	✓	
10	0.974155	✓	
11	0.970701	✓	
12	0.97079	✓	
13	0.848119	✓	
14	0.98401	✓	
15	-0.99998		x
16	0.956772	✓	
17	0.978085	✓	
18	0.982813	✓	
19	0.97902	✓	
20	0.978131	✓	
21	0.974685	✓	
22	0.971058	✓	
23	0.990261	✓	
24	0.9898	✓	
25	0.973368	✓	
26	0.975856	✓	
27	0.972014	✓	

Person	5th Image		
	Value	Accept	Reject
28	0.971886	✓	
29	0.985501	✓	
30	0.971591	✓	
31	0.968107	✓	
32	0.983998	✓	
33	0.986356	✓	
34	0.977923	✓	
35	-0.4524		x
36	0.992816	✓	
37	0.96857	✓	
38	0.336763	✓	
39	0.973878	✓	
40	0.971256	✓	
41	0.970755	✓	
42	0.976669	✓	
43	0.975361	✓	
44	0.978203	✓	
45	0.964415	✓	
46	0.978335	✓	
47	0.977442	✓	
48	0.970062	✓	
49	0.986014	✓	
50	0.94638	✓	
51	0.946405	✓	
52	0.971939	✓	
53	0.989561	✓	
54	0.979579	✓	
55	0.967715	✓	

Person	5th Image		
	Value	Accept	Reject
56	0.968074	✓	
57	0.972723	✓	
58	0.967541	✓	
59	0.96758	✓	
60	0.978711	✓	
61	0.971327	✓	
62	0.979449	✓	
63	0.980278	✓	
64	0.978388	✓	
65	0.979766	✓	
66	0.979058	✓	
67	0.981591	✓	
68	0.9743	✓	
69	0.989666	✓	
70	0.984897	✓	
71	0.968826	✓	
72	0.977751	✓	
73	0.973093	✓	
74	0.989456	✓	
75	0.966586	✓	
76	0.989129	✓	
77	0.975741	✓	
78	0.97928	✓	
79	0.981401	✓	
80	0.975659	✓	
81	0.958121	✓	
82	0.971686	✓	
83	0.968266	✓	

Person	5th Image		
	Value	Accept	Reject
84	0.958672	✓	
85	0.983681	✓	
86	0.973105	✓	
87	0.961202	✓	
88	0.98426	✓	
89	0.820829	✓	
90	0.953731	✓	
91	0.981953	✓	
92	0.892104	✓	
93	0.985038	✓	
94	0.975956	✓	
95	0.846801	✓	
96	0.977443	✓	
97	0.976181	✓	
98	0.985607	✓	
99	0.97666	✓	
100	0.973908	✓	
101	0.987089	✓	
102	0.977097	✓	
103	0.976651	✓	
104	-0.99987		x
105	0.96504	✓	
106	0.973284	✓	
107	0.978526	✓	
108	0.98414	✓	

VITAE

Sawet Somnugpong was born on April 22nd, 1986, in Chiangmai Province. He obtained his bachelor's degree in Computer Science from the Faculty of Applied Science, King's Mongkut University of Technology North Bangkok in 2009.